HydroBlox: AI-Assisted Visual Programming Framework for Enhanced Scientific Reproducibility in Hydrology

Carlos Erazo Ramirez[1,2,*], Ibrahim Demir[1,2]

[1] River-Coastal Science and Engineering, Tulane University
[2] ByWater Institute, Tulane University
[*] Corresponding Author, cerazoramirez@tulane.edu

Abstract

Scientific workflow reproducibility for hydrological and environmental analyses remains a challenge due to the heterogeneity of data sources, analysis protocols, and evolving visualization needs. This study introduces HydroBlox, a client-side browser-based framework that supports the creation, execution, and export of hydrological workflows using a visual programming interface. The platform integrates modular web libraries to perform data retrieval, statistical analysis, and visualization directly in the browser. Two case studies demonstrate the platform: precipitation–streamflow response analysis in the Iowa River Basin and SPI-based drought characterization using a workflow that produces ensemble drought scenarios. Results demonstrate the system's capacity to facilitate reproducible, portable, and extensible hydrological analyses across a range of spatial and temporal scales. The study discusses the architecture, implementation, and capabilities of the system and explores its implications for collaborative research, education, and low-code scientific computing in hydrology.

Software Availability

Name	HydroBlox
Developers	Carlos Erazo Ramirez, Ibrahim Demir
Cost	Free
Software Required	Web Browser
Program Language	JavaScript, HTML, CSS
Platform Access	https://hydroinformatics.tulane.edu/lab/hydroblox

This manuscript is an EarthArXiv preprint and has been submitted for possible publication in a peer reviewed journal. Please note it is currently undergoing peer review for the second time. Subsequent versions of this manuscript may have slightly different content.

1. Introduction

Reproducibility of scientific process is a cornerstone of scholarly progress and yet it remains a persistent challenge in hydrological modeling studies due to an increase in the complexity of computational workflows (Gil et al., 2016; Stagge et al., 2019). The complexity of hydrological systems—spanning diverse spatial scales, forcing mechanisms, and land-atmosphere interactions—requires flexible, yet standardized workflows to ensure transparency and repeatability in research outcomes (Ewing et al., 2024). As hydrological science increasingly adopts computational methods, the ability to design, execute, and reproduce workflows has emerged as a key criterion for scientific credibility (Hutton et al., 2016; Hut et al., 2022). However, computational reproducibility is often halted by fragmented toolchains, proprietary software dependencies, and undocumented data processing steps that create significant barriers in the replication of published results.

Ruiz-Pérez et al. (2016) and Essawy et al. (2018) highlight that the lack of open, shareable workflows impedes the replication of published results, limiting trust in analysis outcomes and model predictions. Calls for formalized workflows and open-source tooling have grown, emphasizing the need for platforms that support consistent execution, metadata preservation, and collaborative extension.

In parallel, advances in user-interface design and web technologies have created new opportunities for lowering the barrier to entry in environmental modeling. Visual programming languages (VPLs), such as those implemented in educational tools and embedded systems, enable users to construct logical workflows through block-based or diagrammatic interfaces without writing code (Kuhail et al., 2021). Within hydrology, such paradigms hold promise for empowering researchers, educators, and practitioners to build and share analyses without extensive software training (Finkenbiner & Semmendinger, 2021).

While significant progress has been made through platforms like HydroShare, which promote metadata preservation and standardized publication (Tarboton et al., 2022; Maghami et al., 2024), these systems often require complex backend infrastructure, local runtime environments, or high levels of scripting proficiency. There is currently a lack of browser-native, modular tools that enable fully visual workflow development and execution within a decentralized, client-side context. Existing workflow management systems such as Apache Airflow, Kepler, or Argo Workflows typically require complex server-side deployment or containerized environments like Docker, which may present a barrier for educational use or field applications. This work introduces HydroBlox, a web-based visual programming framework designed to address this gap. HydroBlox establishes the web browser as an autonomous, high-performance scientific runtime, limited solely by the user machine. The framework is architected around a universal compute manager capable of orchestrating four distinct execution engines enable near-native performance for computationally intensive tasks entirely on the client side. This approach leverages modern web standards for in-browser model execution, local data storage, and offline use and non-blocking parallel execution.

The framework integrates a global data orchestration layer with programmatic access to hundreds of data endpoints from over twenty major agencies described later in the text. By

automating complex Web Services and protocols, the application eliminates the manual friction typically associated with data acquisition. Additionally, HydroBlox introduces a local-first AI assistant utilizing a dual modality of service driven AI and local in-browser inference, ensuring that AI-guided workflow construction and debugging occur with complete data privacy and without external API dependencies. This web-first paradigm enables a cohesive research lifecycle that is instantly shareable as a standalone, offline-capable Web Application.

2. Background and Related Work

2.1. Reproducibility and Open Workflows in Hydrology

Reproducibility remains a central challenge in computational hydrology. Despite widespread use of models and analytical pipelines, many studies lack publicly shareable workflows or clear documentation of data transformations (Demir & Szczepanek, 2017). Hutton et al. (2016) argue that without reproducible methodologies, computational hydrology risks undermining its scientific credibility. Tools like HydroShare (Essawy et al., 2018; Tarboton et al., 2022) and HydroBench (Moges et al., 2022) have made significant strides in enabling reproducibility through hosted environments and standardized benchmarking practices.

Cross-institutional hydrological research increasingly depends on interoperable systems and open data exchange standards. Frameworks such as Open Geospatial Consortium (OGC) Web Services, HydroServer, and the CUAHSI WaterML (Almoradie et al., 2013) specification have enabled broader data sharing (Squividant et al., 2015). The need for accessible, integrable tools is particularly acute for responding to “wicked problems” in climate and water systems that require collaboration across scales and domains (Cushing et al., 2015). Despite the growing emphasis on reproducibility and data sharing, most hydrological workflows remain script-based or confined to legacy desktop applications. There is a need for tools that not only promote transparency but also make workflow construction more approachable and usable in educational and research settings (Merwade & Ruddell, 2012). Visual programming environments have emerged in other fields as a way to address this gap.

2.2. Cloud Services and Browser-Native Paradigms

The hydrological sciences have increasingly adopted cloud-native technologies to meet the demands of large-scale, distributed, and collaborative workflows. Cloud platforms provide scalable infrastructure for data storage, model execution, and multi-user access, making them central to recent advances in hydrology and water resource forecasting (Seo et al., 2019). Initiatives like the Cooperative Institute for Research to Operations in Hydrology (CIROH) have emphasized cloud-native design patterns, using containerization, microservices, and cloud object storage (e.g., Amazon S3) to support operational hydrology at national and regional scales (Burian et al., 2023). These architectures facilitate integration of near real-time data, ensemble forecasting, and advanced Earth observation analytics. Cloud-hosted tools—such as NOAA's Big Data Program (Simonson et al., 2022), Google Earth Engine (Zhao et al., 2021), and NASA's AWS-based data access portals—have become essential to modern hydrological research and decision-making workflows.

However, while cloud-native platforms offer flexibility and computational power, they often introduce significant overhead related to secure authentication, backend configuration, dependency management, and complexity of cloud-specific APIs. For educational use, field

applications, or resource-limited environments, these requirements may present a barrier. Furthermore, myriad existing workflow tools such as Apache Airflow, Kepler, or Argo Workflows—while highly effective for industrial-scale orchestration—typically require a sophisticated backend server environment to manage execution logic and state. This infrastructure requirement can limit the immediate portability and reproducibility of workflows for researchers who lack access to persistent server resources.

The web development ecosystem has matured to support browser-native scientific applications. Technologies such as WebAssembly for in-browser modelling and robust data analysis (Sit et al., 2021; Agliamzanov et al., 2020; Ewing et al., 2024), IndexedDB for dynamic data storage, Service Workers for offline usage, and client-side JavaScript frameworks for visualization. These browser-based systems operate entirely on the client side, requiring no server infrastructure or local installations, and can be distributed as static Progressive Web Applications (PWAs) that support offline use and session persistence (Shahid et al., 2023; Hume, 2017).

The convergence of cloud and browser-native capabilities presents a new paradigm for hydrological tools where cloud-hosted datasets and APIs can be accessed directly from lightweight, browser-executed workflows. This hybrid model reduces friction for tool adoption, improves reproducibility, and expands participation in hydrological computing by accommodating a wider range of users and technical environments. Unlike traditional methods that separate the data storage from the computational interface, this web-first approach enables a "zero-install" environment where the user's local hardware executes compiled scientific code at near-native speeds. By leveraging these browser-native capabilities, it becomes possible to bridge the gap between authoritative global data repositories and immediate, high-performance analytical modeling.

2.3.Visual Programming in Science

Visual programming languages (VPLs) use graphical representations—such as blocks, nodes, or flowcharts—to define program logic and task sequences. These systems are widely used across science, engineering, and education to simplify complex processes and improve transparency in execution. A systematic review by Kuhail et al. (2021) classifies VPLs into block-based (e.g., Scratch, Blockly) and diagram-based (e.g., Simulink, Node-RED) paradigms, each enabling end users to construct executable workflows without direct scripting.

In educational settings, block-based languages have demonstrated strong benefits for introductory computing and STEM (Science, Technology, Engineering and Mathematics) education. Tools like MIT Scratch, App Inventor, and Snap! support foundational learning in logic, algorithms, and event-driven programming, often improving student confidence and engagement (Stolpe & Hällström, 2023). Beyond education, visual programming has gained traction in automation, robotics, and embedded systems, where interfaces like Simulink (MATLAB) (Karris 2016), LabVIEW (National Instruments) (Kodosky, 2020), allow users to define signal processing, control logic, or real-time hardware operations.

In data science and machine learning, node-based platforms like Knime (Feltrin, 2015), Orange, and RapidMiner (Verma, et al., 2014) enable visual pipeline design for data preprocessing, model training, and evaluation. These systems allow analysts to link modular components—such

as filters, classifiers, or visualizations—into reusable, interpretable workflows. Similar principles are applied in industrial automation (e.g., Node-RED) and geospatial processing (e.g., ArcGIS ModelBuilder, Google Earth Engine GUI), where task chains are visually represented to assist non-expert users.

The scientific community has also recognized the role of VPLs in improving workflow reproducibility. Workflow management systems such as Kepler, Taverna, and Apache NiFi offer visual environments for composing complex, multi-stage processes across disciplines including bioinformatics, climate modeling, and computational chemistry. These tools support documentation, version control, and dependency management through visual representations, facilitating collaboration and repeatable analyses (Gil et al., 2007; Deelman et al., 2009).

In hydrology and environmental science, the adoption of VPLs has been limited. Most existing tools rely on either point-and-click desktop interfaces or scripting through Python, R, or MATLAB. However, work by Finkenbiner and Semmendinger (2021) illustrates the potential of visual workflows in sensitivity analysis for hydrological models. While platforms like Tethys (Swain et al., 2016) and HydroShare (Horsburgh et al., 2016) support workflow reproducibility, they typically require backend infrastructure and are not designed for generalized visual programming. There remains a gap for client-side, modular VPLs tailored to hydrological research and education.

2.4.Web-based Hydrological and Environmental Tools

Building on these advances in browser-native architectures and visual workflow paradigms, several web-based hydrological and environmental toolkits have emerged that encapsulate data access, analysis, and visualization into reusable client-side libraries and platforms. HydroSuite is a collection of web-based hydroinformatics tools, portals, benchmark datasets, and community portals that aim to improve web-based development of hydrology and environmental workflows, both browser based and server side (HydroSuite, 2024). It provides a large collection of libraries that allow connection to a varied set of data sources, analytical engines for analysis and visualization, tools for exporting data and providing information through portals, and creates a synergic environment with the available tools from the user, exposed to their client-side technology.

HydroLang is a web-based, open-source library designed to facilitate hydrological and environmental data processing, analysis, and visualization (Erazo et al., 2022). It offers a collection of functions implemented in JavaScript, enabling users to interact with various datasets and APIs without the need for extensive software installations. The library supports multiple functionalities, including statistical computations, hydrologic functions, and interactive visualizations, making it a flexible resource for researchers, practitioners, and educators. The library's architecture is modular, encouraging extensibility and ease of use through its predefined functions and adaptable workflow. HydroLang provides access to multiple data sources, including publicly available hydrological databases and APIs, enabling users to retrieve, manipulate, and visualize datasets efficiently. Its lightweight nature and web-based execution make it particularly suitable for real-time applications (Erazo et al., 2023)

HydroCompute serves as the core orchestration layer for the platform, providing an open-source, client-side library designed to support high-performance data processing in hydrology (Erazo et al., 2024). The library leverages modern web standards—including Web Workers, WebGPU, and WebRTC—to enable the parallel execution of scientific computations directly within the browser. Its architecture manages the lifecycle of every computational task through a standardized Input → Execute → Save model. When a workflow is triggered, HydroCompute traverses the dependency graph, isolates the required data, and dispatches it to the appropriate runtime environment. This includes managing the instantiation of different computing engines and languages. By abstracting the complexity of these diverse environments, HydroCompute ensures that data lineage is preserved and that heavy computational loads are executed asynchronously without blocking the main user interface.

2.5. Intelligent Interfaces and AI Integration in Environmental Research

Recent advances in artificial intelligence (AI) and natural language processing (NLP) have enabled new types of interactive interfaces for scientific computing (Pursnani et al., 2025). In particular, large language models (LLMs) are now being explored to support code generation (Pursnani et al., 2024), workflow assistance, and automated interpretation of results for hydrological research, education and operations (Sajja et al., 2025), as well as benchmark datasets for the usage of LLMs in hydrology (Kizilkaya et al., 2025). These developments aim to reduce technical barriers and improve accessibility, especially for researchers who may not be familiar with traditional programming environments (Mishra et al., 2023; Luan et al., 2022; Haristiani, 2019).

In environmental and geoscience domains, AI-driven interfaces remain limited but are gaining attention. For example, tools such as EarthAI and Google Earth Engine Explorer have begun integrating machine learning support for automated classification and search. In broader data science contexts, platforms like Jupyter AI and OpenAI Codex have demonstrated the ability to assist in writing code, querying datasets, and explaining statistical outputs through natural language interaction (Perkel, 2023).

While hydrology-specific applications are still in early stages, rule-based decision support systems (e.g., within HydroShare or OpenDA (Ridler et al., 2014)) have provided foundational steps toward AI-guided workflows. These tools typically support task selection, parameter tuning, or metadata management based on user-defined rules (Essawy et al., 2018; Maghami et al., 2024). The integration of LLMs promises to expand these capabilities by enabling dynamic assistance during workflow construction, parameter selection, and interpretation of hydrological indicators.

Combining visual programming with AI-guided assistance represents a promising path forward (Feng & Yan, 2024). Intelligent interfaces can help users—particularly those in training or applied fields—understand the role of each processing step, suggest next actions, or auto-complete workflow components based on contextual goals. These capabilities align with the broader trend of augmenting scientific tools with AI to support reproducibility, lower entry barriers, and accelerate exploratory analysis (Toshniwal et al., 2023; Wagner et al., 2022).

2.6. Proposed Framework

The objective of this work is to develop a browser-based framework for constructing, executing, and sharing hydrological workflows through a visual programming interface. The framework

addresses limitations in existing hydrological tools through a decentralized, client-side architecture built on modern web technologies. Its primary goals are to: i) provide a modular visual environment for composing hydrological, geospatial, and data acquisition workflows; ii) enable complete in-browser execution without backend infrastructure or local software installation; iii) support extensibility across multiple runtimes; iv) facilitate reproducibility and portability through exportable standalone workflows and web apps; and v) support both hydrological research and educational applications through interactive and workflow-driven computing.

3. Methodology

3.1. System Overview

HydroBlox is a client-side web application designed for modular extensibility and execution entirely within the browser. Operating without a backend server, the platform relies on open web standards to provide a responsive and portable interface across devices. The main purpose of the application is to enable a visual programming paradigm that caters to users in hydrology and beyond through an extensible framework, enabling the use of multiple programming languages and scopes for generating reproducible analysis.

3.2. Architecture Layers and Responsibilities

The application is organized into three architectural layers: interface components, core system modules, and external execution libraries. Interface components include the user-facing elements used to construct and inspect workflows, such as navigation bars, workflow blocks, the canvas, and visualization tools. Core modules manage workflow orchestration, including state and dependency tracking, dynamic block instantiation through a centralized item factory, execution coordination, and client-side persistence of intermediate and final results. External libraries provide the domain-specific computational and rendering functionality invoked during execution. Table 1 summarizes these architectural components and their relationships, as illustrated in Figure 1. Workflows are represented as visual graphs of interconnected blocks corresponding to tasks such as data retrieval, transformation, analysis, and visualization. Internally, each workflow is encoded as a Directed Acyclic Graph (DAG), where nodes represent workflow blocks and edges define dependencies between input and output connections. The graph is maintained dynamically through an adjacency-list structure that updates as users modify the canvas. To ensure execution stability, cycles are prevented during connection validation, while disconnected nodes may execute independently if their data requirements are satisfied.

Execution is coordinated through specialized manager modules. A Connection Manager maintains workflow edges, a State Manager tracks workflow development states, and an Execution Manager traverses the DAG in topological order using depth-first search before dispatching tasks to the appropriate runtime environment. A Running Manager coordinates interface updates and execution feedback, while a Results Manager handles rendering, visualization, and export of workflows as standalone web applications. An integrated AI Assistant supports workflow construction by processing user input and generating recommendations, insights, and workflow suggestions. The following sections describe the principal components of the HydroBlox architecture and their roles within the execution framework.

Table 1. Responsibilities of each implemented manager on the platform.

Category	Module / Component	Responsibility
User Interface	Interface Components	User interface templates including navigation bars, modals, workflow canvas, and result panels
Core Module	Items / Blocks	Definition, instantiation, and configuration of draggable logic blocks and their input–output interfaces
Core Module	Functionality	Management of workflow state transitions, dependency resolution, task execution, and results aggregation
Core Module	Database Integration	Persistent client-side storage of workflow state, intermediate data, and results to support reproducibility
Core Module	Web App Exports	Packaging of workflows and results into standalone Web Application bundles
External Library	HydroSuite & Code Blocks	Execution and rendering logic provided by different engines

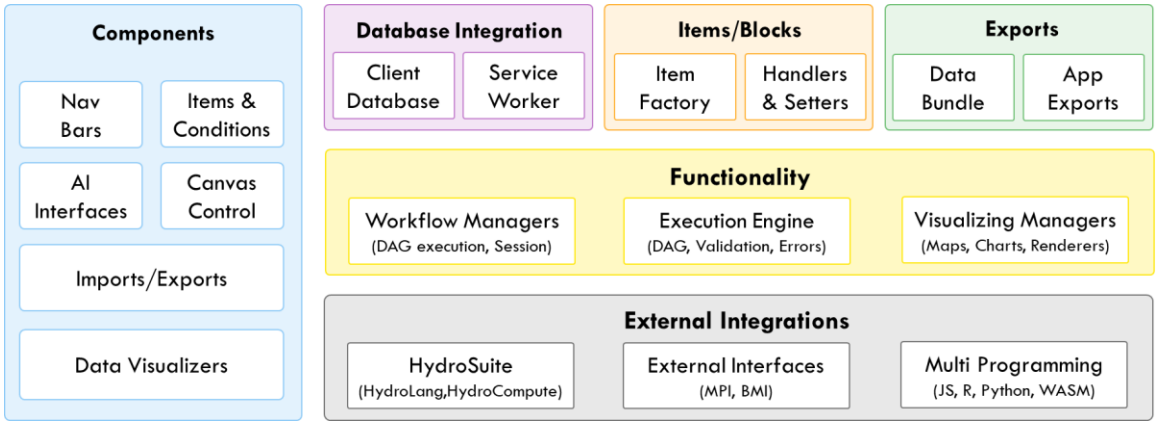

Figure 1. Architecture diagram of the platform, created with and scalability with capability to run R, Python, JS, WASM and new libraries to be readily added through a message passing interface (MPI) or basic modelling interface (BMI) or declarative function paradigm.

3.3. Workflow Authoring in the Canvas

3.3.1. Block Construction

Functional logic in the canvas is represented through modular blocks, where each block encapsulates a discrete operation such as data acquisition, analysis, visualization, or logical control. Users construct workflows by dragging blocks from a component palette onto a grid-based infinite canvas and connecting them through input and output ports. Each block is instantiated through a centralized factory system using a predefined schema that defines its identifier, type, configuration parameters, execution state, spatial position, and permitted connections. Connections between blocks are maintained by the Workflow Manager, which validates graph consistency, updates the internal DAG, and prevents invalid or cyclic dependencies in real time.

Blocks are visually rendered using absolute positioning with snapping and zoom-aware scaling. Each block contains a header, connection ports, and a configuration interface accessible through direct interaction. Figure 2 highlights an example setter window for different block types.

Configuration parameters are dynamically generated from the underlying function definitions and include argument fields, default values, inline descriptions, and dataset previews when applicable. Workflow states and configuration data are automatically synchronized with local storage to preserve persistent sessions. The framework supports both simple and advanced execution patterns through specialized control structures, including conditional branches, iterative execution nodes, mapping operations, and aggregation blocks for combining multiple data streams. Moreover, a set of connection blocks enables communication with processes running on local or external machines through WebSockets and real-time communication protocols (Ramirez et al., 2024), allowing users to create workflow blocks that interface directly with external computing nodes. To ensure extensibility, blocks are dynamically generated from modular libraries integrated through an abstraction layer. This mechanism enables automatic extraction of exposed functions and generation of corresponding visual components while maintaining compatibility with external APIs through a standardized schema and message-passing interface.

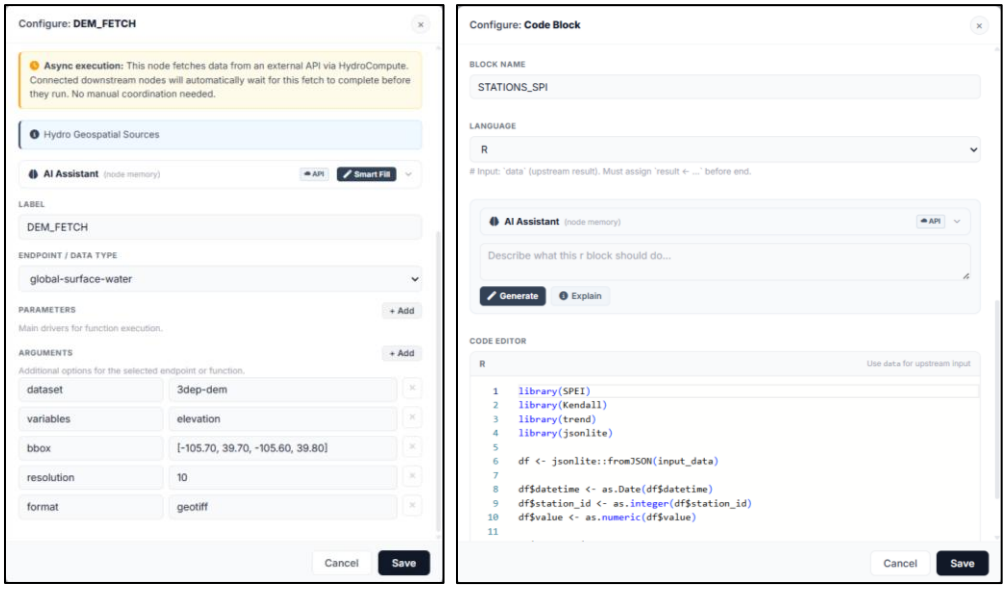

Figure 2. Example of the settings window for different blocks. Users can edit workflow settings using a menu for options that supports the execution based on the function definition is shown.

Functionally, blocks are organized into three primary domains: data acquisition, analysis, and visualization. Other blocks include logic, external process connectors, and helper modules. The data acquisition layer leverages the integrated HydroLang engine, which provides access to numerous national and international data providers and configurable retrieval endpoints. Additional ingestion blocks support user-defined or local datasets. The analysis layer includes hydrological modeling, statistical analysis, machine learning routines, and custom execution environments supporting JavaScript, Python, and R code injection. Computationally intensive tasks are accelerated through WebAssembly integration, discussed further in Section 3.6. Visualization blocks expose configurable rendering interfaces for presenting workflow outputs and analytical results.

3.3.2. Workflow Modeling and Execution

Once items are placed on the canvas, the system builds an internal Indexed DAG where nodes represent functional units and edges define computational dependencies (Figure 3). This structure leverages the browser database as a shared state store to facilitate cross-engine dependency resolution. The architecture enables different runtime environments to asynchronously wait for and consume results from one another, preserving data lineage across workflows composed of heterogeneous programming languages and execution modalities. Upon initiation via the Run command, the State Manager transitions the interface into a locked running mode, evaluates dependencies across the Indexed DAG, identifies executable nodes, and schedules them for parallel dispatch.

An example workflow composed of heterogeneous execution blocks is shown in Figure 4. Data retrieval items, in this case 3DEP datasets for topographic features (USGS, 2023) are subsequently preprocessed using HydroLang's geoprocessor module, leveraging GDAL (GDAL/OGR, 2023) to reproject the digital elevation model (DEM) from EPSG:5070 to EPSG:4326. The processed outputs are then connected to visualization blocks, specifically map and georaster layer components, to explicitly declare data dependencies within the workflow. After execution through the Run command, the outputs become available for visualization and inspection in the results mode, as illustrated in Figure 4, where both the raw and reprojected datasets are displayed simultaneously on the map.

The execution control logic of the main engine is formalized in Figure 5 through pseudocode definitions of workflow management and execution states. These algorithms codify the lifecycle of a workflow execution, including dependency evaluation over the Indexed DAG, batching of executable nodes, parallel task dispatch across runtime backends, state synchronization, and completion signaling.

3.3.3. Multi-runtime Execution and Code Blocks

To support the diverse methodological requirements of the hydrological community, the platform explicitly enables the integration of custom user-defined code. While the visual environment provides a comprehensive library of standard workflow blocks, research applications frequently require specialized statistical algorithms, experimental methods, or the reuse of legacy computational models. By supporting the execution of raw Python, R, JavaScript, and C++ modules compiled through WebAssembly, the framework bridges the gap between visual programming and conventional scripting environments. This approach allows researchers to leverage existing scientific software ecosystems without rewriting established codebases, ensuring that the platform remains sufficiently flexible to accommodate emerging analytical techniques and domain-specific workflows.

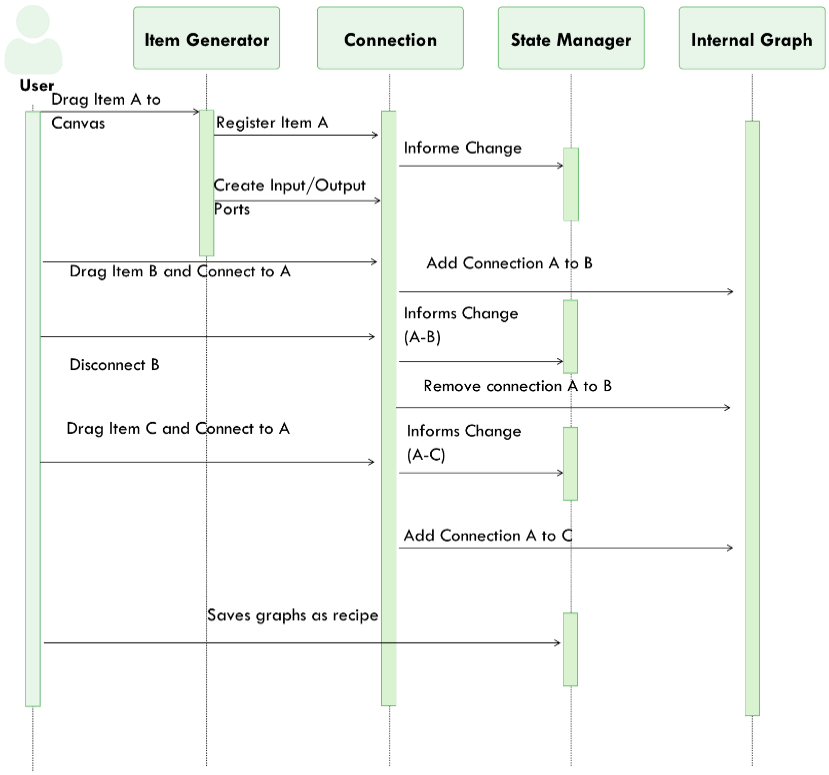

Figure 3. Sequence diagram on the execution and declaration of items. Upon a user placing an item (block) in canvas, the actions described are triggered. In this context, a blocks A, B and C are declared based on type and the data flow.

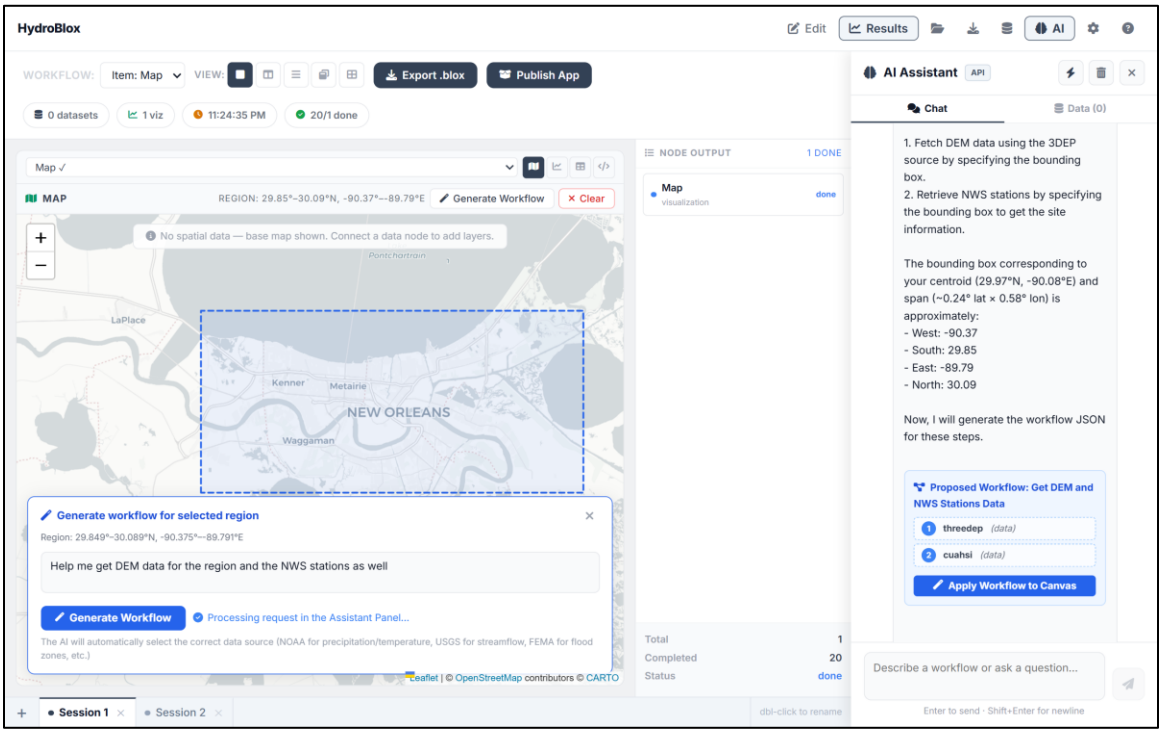

Figure 4. Example on the declaration of items and execution of workflows in running mode.

Algorithm 1 WorkflowManager Core Functionality

```
function ManageWorkflows
    Load workflows from local storage and database
    Apply workflows to canvas if needed
    Listen for UI events (item rename, connection changes, zoom)
    Sync canvas items with workflows
    for all new canvas items do
        if connected to existing workflow then
            Add to workflow
        else
            Create new workflow
        end if
    end for
    for all deleted or renamed items do
        Update workflows and connections
    end for
    Save updated workflows to local storage and database
end function
```

Algorithm 1 Workflow Execution Algorithm

```
function ExecuteWorkflow
    Initialize processed set: 𝒫 ← ∅
    Load all workflows: 𝒲 ← set of all workflows
    for all workflow w ∈ 𝒲 do
        Extract items I ← w.items
        Separate visualization items V ← {i ∈ I | i.type = visualization}
        Filter executable items E ← I \ V
        for all item i ∈ E do
            if i has result in database and parameters unchanged then
                𝒫 ← 𝒫 ∪ {i}
            end if
        end for
        while exists i ∈ E \ 𝒫 such that all d ∈ i.deps are in 𝒫 do
            Prepare function configuration f_i
            Submit f_i to compute engine (JavaScript or WASM)
            Wait for result and transform if needed
            Save result to database
            𝒫 ← 𝒫 ∪ {i}
        end while
        if V ≠ ∅ then
            Emit visualization event for items in V
        end if
    end for
end function
```

Figure 5. Pseudocode execution for the workflow and executor managers where they both sync through the workflow manager, that is continuously checking if items have ran, finished, or were available in the database.

Computation is delegated to specialized runtime environments according to block type: i) Python nodes execute through Pyodide in dedicated workers with access to scientific libraries such as NumPy, Pandas, RasterIO (Pyodide, 2024); ii) R nodes utilize WebR for statistical computing (Ooms, 2024); iii) JavaScript blocks and HydroLang functions execute within standard Web Workers; and iv) WebAssembly modules execute compiled binary routines for high-performance tasks. The Executor orchestrates this multimodal concurrency, ensuring that independent workflow branches execute simultaneously without interference. As tasks complete, execution states are reflected directly within the interface through color-coded indicators representing queued, failed, and completed operations, thereby providing immediate visual feedback and signaling the availability of processed artifacts for downstream inspection.

3.4. Visualization and Results

HydroBlox supports in-place visualization of computational outputs within workflow blocks using modular analysis and rendering components. The example results developed in Section 3.3.2 is shown in Figure 6. Results are displayed directly inside each block and can take the form of tables, charts, or maps. Visualizations are defined through configuration-based specifications that link data outputs to visual elements, enabling automatic rendering of time series, statistical summaries, and geospatial data.

The visualization pipeline is fully client-side and designed to maintain interactivity during execution. Computational tasks and data loading are handled asynchronously to prevent blocking the user interface, allowing users to continue interacting with the workflow even when processing large datasets or external data sources. Outputs can be explored and exported in common formats such as tabular data, images, or geospatial files, supporting downstream analysis.

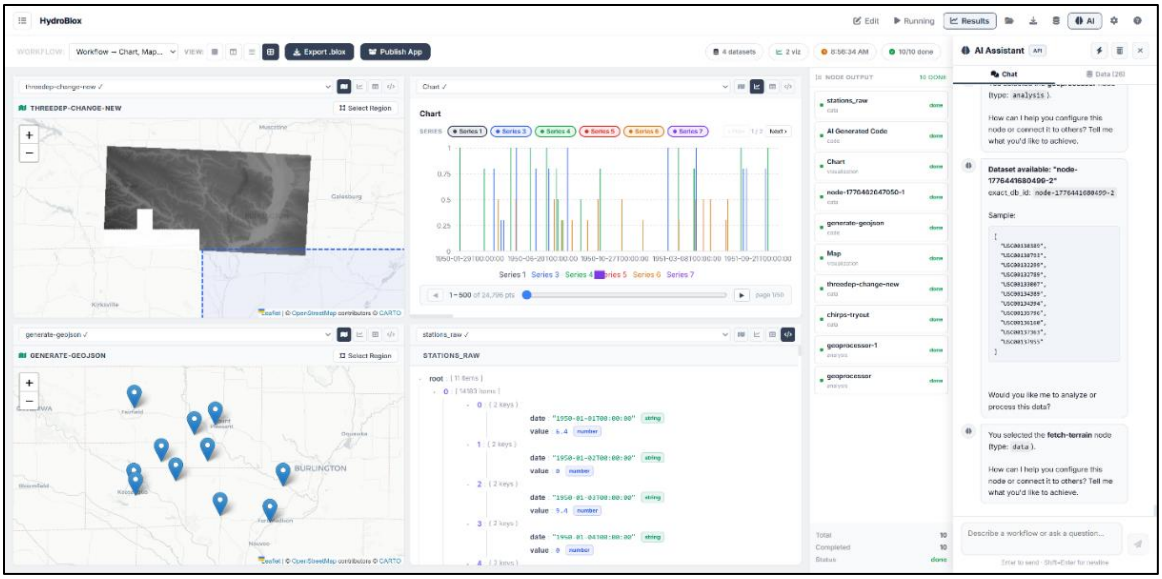

Figure 6. Result space showcasing a control panel, visualization of maps, tables, and charts; multi-modality has been implemented to account for visualization outputs required by the end user.

3.5. Reproducibility and Workflow Recipes

The platform supports full workflow export and import using serialized “recipes.” Each recipe stores all data needed to reconstruct a workflow, including block configurations, positions, connections, data links, and metadata such as timestamps, authorship, and versioning (Figure 7). Recipes are encoded in JSON and shared as .blox files. Export and loader modules handle serialization and deserialization, restoring both the visual and logical workflow structure, including precomputed results when available. The platform also supports drag-and-drop recipe import and browser-based session persistence.


```
{
  "id": "session::session-1777926849834",
  "name": "Session 1",
  "savedAt": 1778190715163,
  "nodes": [
    {
      "id": "node-1777303380804-4",
      "type": "analysis",
      "itemName": "geoprocessor",
      "x": -256.5,
      "y": 308,
      "status": "done",
      "settings": {
        "itemName": "CLIP_DATASETS_SE_IOWA",
        "component": "geoprocessor",
        "selectedFunction": "clipGeo",
        "parameters": {
          "source": "clipGeo"
        },
        "arguments": {
          "west": -92.92236,
          "south": 40.5472,
          "east": -90.10986,
          "north": 42.14711,
          "bounds": "[-92.92236,40.5472,-90.10986,42
            .14711]"
    {
      "id": "node-1777320837154-4",
      "type": "trigger",
      "itemName": "Parallel Map",
      "x": -316.6,
      "y": 209.9,
      "settings": {
        "itemName": "Parallel Map",
        "type": "trigger",
        "data": [
          "node-1777321455274-0",
          "node-1777473488466-1"
        ],
        "conditionLeft": "",
        "conditionOperator": "equals",
        "conditionTargetType": "value",
        "conditionRightValue": "",
        "conditionRightInput": "",
        "conditionFieldPath": "",
        "triggerType": "parallel_map",
        "pmSourceKey": "",
        "pmTargetParam": "year",
        "pmMerge": "array",
        "pmNamedSource": "",
        "pmGcEnabled": true,
        "pmInputs": [],
```


Figure 7. Example of the reproducible recipe saved as a .blox JSON object defining an item, as well as the connections within.

3.9. AI-Assisted Workflow Generation

The platform includes an AI-assisted workflow intelligence layer integrated with the visual programming environment and execution engine and is aware of workflow state, execution semantics, and function schemas, enabling it to generate, validate, and modify executable workflows from natural-language input (Figures 8 and 9). It operates under a defined set of system rules that constrain its behavior and specify permitted actions, ensuring consistent, schema-compliant workflow construction. The AI is execution-aware but computation-agnostic: numerical modeling, statistical analysis, and geospatial processing remain handled by deterministic workflow blocks. Its role is focused on workflow composition, orchestration, and interpretation. During inference, the system maintains and incrementally refines an internal contextual representation of the session, progressively narrowing user intent into more specific actionable steps. It continuously updates this context using the current workflow state—including nodes, connections, execution status, parameters, and stored outputs—allowing it to reuse results, diagnose failures, and propose targeted refinements. The platform supports two AI execution modalities: service-based inference through external large language model APIs (e.g., OpenAI, Anthropic), and fully local in-browser inference through WebLLM (MLC AI, 2024). This dual-modality design allows users to select either cloud-connected or self-contained execution depending on connectivity, privacy, and reproducibility requirements. The AI layer supports the full workflow lifecycle, including generating structured workflow graphs from natural-language descriptions, providing schema-aware configuration guidance, assisting with execution-time error diagnosis, and summarizing workflow outputs after completion. All AI-generated modifications require explicit user approval before being applied to the canvas. By integrating AI directly within the workflow context, the platform extends visual programming into an interactive modeling environment while preserving transparency and user control over analytical processes.

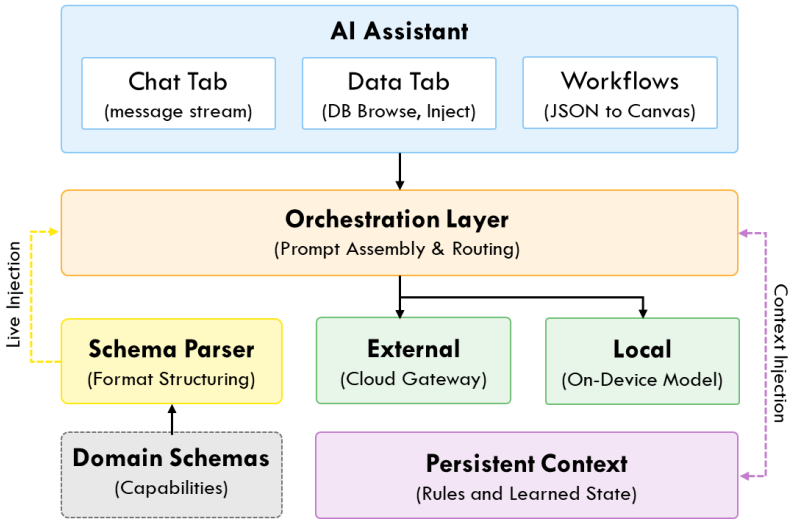

Figure 8. Five-layer architecture that translates natural language queries into executable workflows by routing them through an orchestration controller to local or cloud inference engines, all grounded by persistent memory and dynamic domain schemas.

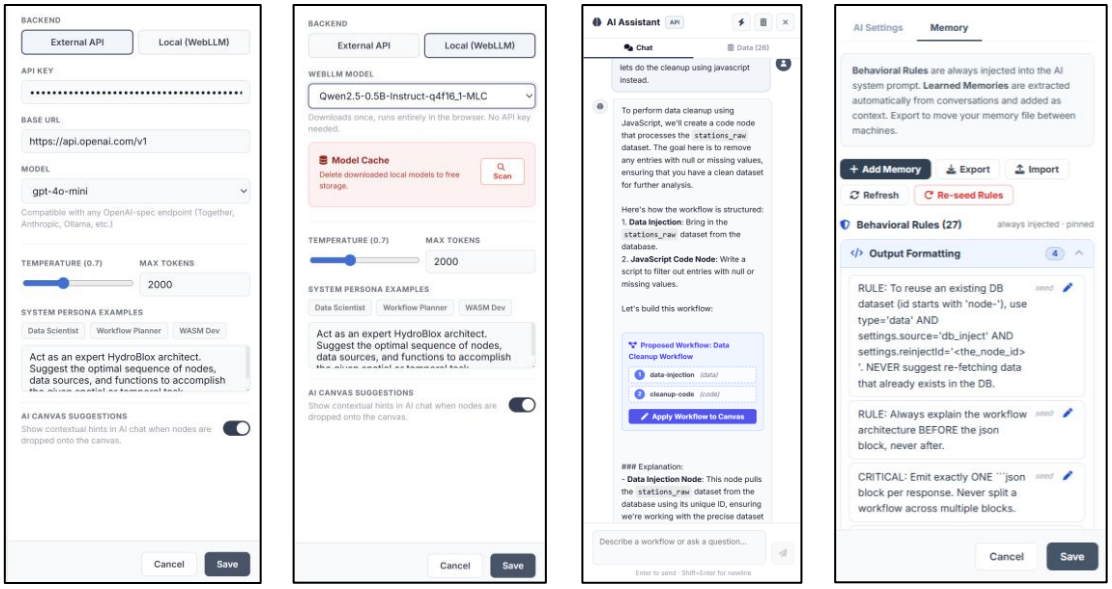

(a) (b) (c) (d)

Figure 9. (a) Interface that manages the AI assistant (b) selection of external or local modalities (c) response on a query from the LLM to apply nodes to canvas and (c) sample of memories injected into the LLM during inference.

3.10. Web Application Export

The system supports exporting fully executable workflow results as standalone web bundles. This capability packages an entire session—including block configuration, execution logic, visual layout, and results—into a self-contained artifact that can be shared, opened, and executed offline in a modern browser. The exported bundle includes the workflow interface, execution and rendering logic for outputs such as charts, maps, and tables, along with serialized configurations and datasets required to reproduce the analysis. The exported package functions as a portable web application that preserves interactivity and client-side execution without external dependencies. Users open the bundle directly in the browser and interact with the saved workflow in the same way as within the original environment. Exported workflows can be re-imported into the platform for modification or re-execution, supporting iterative analysis and reproducibility.

For offline-first use cases, the export can be packaged as an installable Progressive Web Application, enabling local installation and offline access through standard browser capabilities. This supports educational, collaborative, and archival scenarios where workflows must operate without connectivity. The export mechanism decouples workflows from the runtime environment, enabling long-term preservation and sharing without requiring cloud infrastructure or continuous access to the platform.

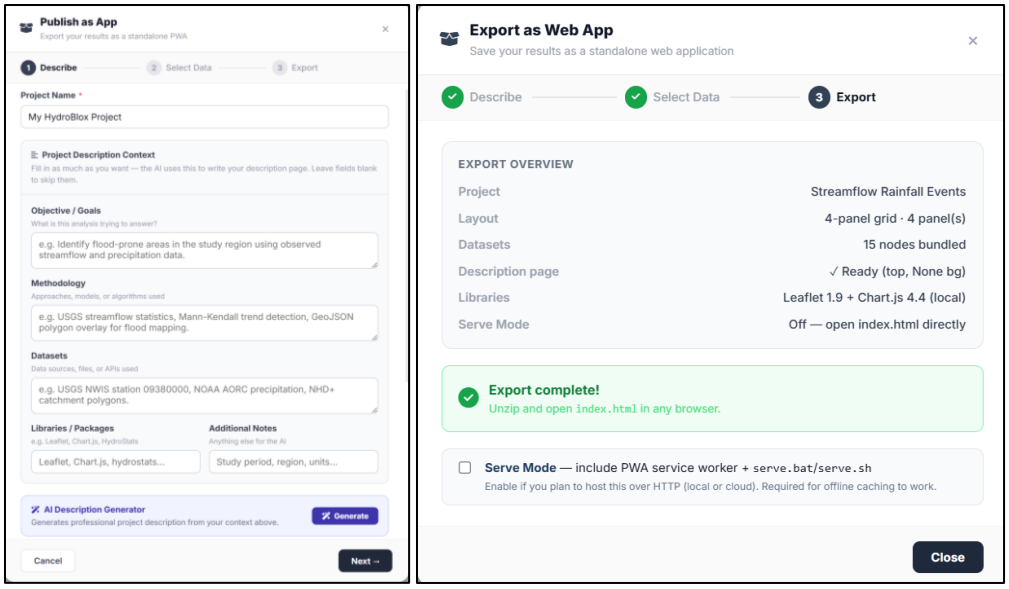

Figure 10. Sample of the app publishing screen. It allows the user to choose template for exporting, data linkage, and exporting as a standalone web app.

4. Results

4.1. Performance of Workflows

To evaluate the platform under realistic usage conditions, we benchmarked representative workflows from the application's workflow library, which includes hydrological analysis, water-quality assessment, climate and time-series analysis, forecasting and machine learning, and spatial analysis using gridded datasets. Selected workflows reflect common end-to-end browser-native operations, including data retrieval, in-browser processing, and interactive visualization without server-side analytical execution.

Evaluation workflows were grouped into three categories based on computational complexity and data intensity: (i) low-complexity transactional workflows involving lightweight data retrieval and visualization of small JSON payloads; (ii) CPU-intensive analytical workflows combining large-volume requests, multi-stage processing across JavaScript, WebAssembly, Python, and R runtimes, and interactive chart rendering; and (iii) spatial processing workflows involving raster interpolation, clipping of multi-band GeoTIFF datasets, R-based value extraction, and interactive map rendering (Table 2). Each workflow integrates multiple platform components to emulate realistic user behavior, including chained operations, parallel execution, and iterative processing. Performance was measured as end-to-end elapsed time from workflow initiation to completion of the final rendered output. Measurements include data retrieval and parsing, runtime execution, inter-worker communication, and local persistence operations such as IndexedDB access. Experiments were conducted in Google Chrome on consumer-grade hardware running Windows OS with 32 GB RAM using a single browser session. The results include the worst-case scenario using Mozilla Firefox as runtime, however, these were tested in Google Chrome, Edge, and Safari browsers.

Table 2. Computational characteristics and performance metrics of representative evaluation workflows.

Workflow	Description	Dataset Size (MB)	Total Execution Time (ms)
WF1	Simple: Fast data load and JSON output	0.90	1,279
WF2	Medium: Dataset 1990s–2023 (800K+ points), JS processing, Python analysis, chart visualization	450	23,717
WF3	Complex: CHIRPS raster processing, JS reproject/clip, R code to extract values, map rendering	660	233,057

Execution time scaled predictably with dataset size and computational complexity. The transactional workflow (WF1) processed a 0.90 MB JSON payload in approximately 1.3 s (1,279 ms). The analytical workflow (WF2) processed approximately 450 MB of data (~800K+ points spanning the 1990s–2023), including JavaScript preprocessing and Python-based analysis, completing in ~23.7 s (23,717 ms). The spatial workflow (WF3), involving memory-intensive raster reprojection, clipping, R-based extraction, and interactive map rendering across ~660 MB of data, completed in ~233 s (233,057 ms) (Figure 11). These results demonstrate that substantial environmental analyses can be executed entirely within a modern browser, with performance primarily influenced by data volume, processing complexity, and client-side runtime overhead. Python and R execution blocks introduce a one-time initialization cost because WebAssembly binaries and supporting packages must first be loaded into the execution environment. Subsequent executions benefit from service-worker caching, reducing repeated initialization overhead and improving warm-cache performance relative to cold-start runs.

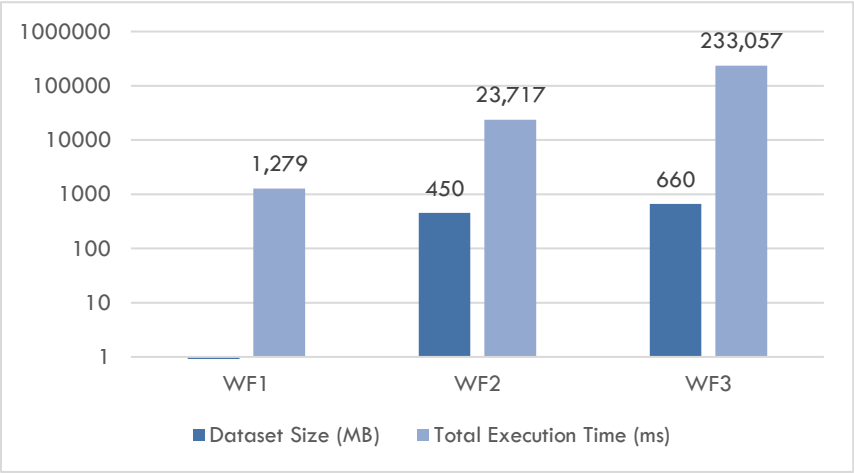

Figure 11. Total execution time (in milliseconds) for the three representative workflows. A logarithmic scale is utilized to visualize the order-of-magnitude differences between the transactional (WF1), analytical (WF2), and spatial processing (WF3) tasks.

Within this browser-native architecture, performance is constrained primarily by memory allocation, serialization, and local storage overhead rather than network throughput. This behavior is reflected across workflows: WF1 is dominated by lightweight parsing and rendering, WF2 by large-scale ingestion and multi-stage analysis, and WF3 by memory-intensive raster processing and large-object movement through the rendering pipeline.

To identify runtime bottlenecks, we profiled representative executions using browser performance tracing (Figure 12). The traces indicate that the core application logic is largely non-blocking; however, measurable latency is introduced by the lifecycle of processed data, particularly: (1) transfer of results from worker threads to the main thread, (2) serialization into storage-friendly formats, and (3) persistence and retrieval from IndexedDB for rendering. During high-volume ingestion phases, serialization and local database I/O (e.g., operations labeled *handleWorkerMessage* and Blob creation) account for a substantial fraction of main-thread activity (approximately 18% under peak ingestion conditions). In addition, memory usage exhibits characteristic spikes followed by browser-triggered garbage collection events; for example, WF2 shows rapid heap expansion peaking near ~510 MB before stabilization. These observations suggest that performance in large workflows is governed primarily by in-browser memory management and storage I/O overhead rather than network latency or blocking computation.

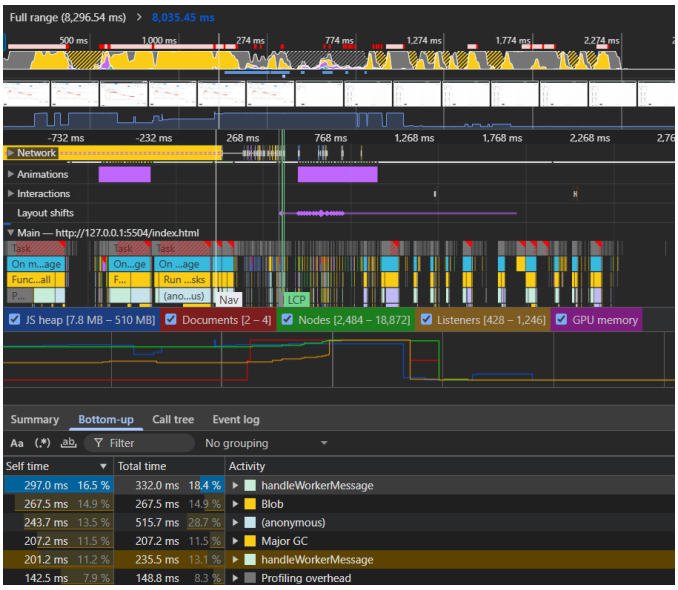

Figure 12. Chrome DevTools performance trace showing main-thread activity and memory usage during execution of Workflow 2 (USGS Data Analysis). The JS heap peaks near ~510 MB as processed data is retrieved from IndexedDB. Prominent handleWorkerMessage and Blob creation events indicate that latency is dominated by serialization and data transfer between local storage and the rendering engine rather than blocking computation.

4.2. Performance of the AI Component

We evaluated the AI-assisted workflow generation component using a deterministic benchmarking engine that produced a reproducible suite of 121 independent queries. Queries were derived from:

(1) documentation-aligned unit tests covering supported data sources, functions, visualizations, and code templates; (2) production workflows from the platform's example library; and (3) synthetic multi-stage hydrological, geospatial, and statistical pipelines. To ensure comparability, all tests were executed in a headless environment with the inference state reset prior to each query, enforcing zero-shot evaluation conditions.

Queries were grouped into four categories representing increasing workflow complexity and distinct assistant behaviors: (i) easy—single-block or minimally parameterized requests; (ii) medium—multi-block workflows requiring correct dataflow and parameter consistency; (iii) complex—multi-stage pipelines spanning acquisition, analysis, and visualization with stricter requirements for graph topology, inter-block compatibility, and cross-runtime execution (e.g., JavaScript with Python/R); and (iv) chat reasoning—conversational support tasks evaluating domain-aware guidance and explanatory capabilities rather than strict workflow construction.

For each query, model output was validated against a ground-truth specification derived from platform block schemas and reference workflows. Validation consisted of three levels: (1) schema-level checks verifying JSON structure, block types, and parameter constraints; (2) topology-level checks evaluating required nodes, dependencies, and permissible dataflow connections; and (3) token-/logic-level checks for code-bearing blocks (Python/R/JS), ensuring required library calls, inputs/outputs, and constrained logic elements were present and computationally consistent.

Workflow outputs were scored on a normalized scale from 0 to 1 based on the fraction of required elements correctly generated. Outputs failing mandatory structural constraints or producing invalid JSON received a score of 0, while partial matches received proportional credit based on node, parameter, topology, and logic coverage. Chat reasoning queries were evaluated separately using relaxed keyword-based scoring, where credit was assigned according to required domain keyword coverage.

Performance is summarized using three complementary metrics: (i) overall accuracy—the mean normalized score within each query category, reported as a percentage; (ii) syntactic precision—the proportion of structurally valid outputs independent of workflow correctness; and (iii) functional recall—the extent to which required functional elements, including nodes, parameters, topology, and constrained logic, were successfully generated. Reported inference times represent end-to-end latency per query. For server-side models, this includes network transmission and remote processing, whereas for local/client-side models executed through WebLLM or similar runtimes, latency reflects on-device inference and therefore depends on user hardware and browser capabilities. The results of the evaluation are explained in Table 3 and Figure 13.

Across the queries, server-side models achieved the highest overall functional correctness. GPT-4o Mini provided the strongest balance of accuracy and functional recall across categories, while GPT-3.5-Turbo maintained high syntactic precision through consistently well-formed outputs. Client-side models showed lower functional correctness under the strict single-shot evaluation protocol but often retained competitive structural compliance, indicating that many failures resulted from incomplete functional elements rather than invalid workflow structure.

Lightweight local models generally provided faster inference, whereas larger local models improved performance on complex workflows at the cost of increased latency. Zero scores observed for some local models in the Easy/Medium/Complex categories primarily reflect the strictness of the evaluation framework, where omission of mandatory elements substantially reduced normalized scores. Qualitative inspection indicates that many outputs contained partially correct workflow scaffolds that would likely converge through iterative multi-turn interaction, which more closely reflects the assistant's intended in-application usage. Consequently, the benchmark serves as a reproducible measure of zero-shot workflow construction and schema adherence while highlighting the importance of iterative feedback for improving practical success rates.

Table 3. Evaluation across the different categories of test examples used to assess the LLMs. For OpenAI models, the reported time reflects end-to-end request latency, including network transmission and server-side processing. For client-side and local models (e.g., WebLLM), the reported time corresponds to on-device inference only and is therefore dependent on the user's hardware.

Model	Easy (%)	Medium (%)	Complex (%)	Chat Reasoning (%)	Avg Inference (ms)
GPT 3.5-Turbo*	53.8	15.4	12.5	75	3183
GPT4o Mini*	53.8	30.8	12.5	75	3452
LLama 3.2 1B	21.3	0	0	55	5121
LLama 3.2 3B	26.3	0	0	55	4761
Phi 3.5 Mini	27.5	0	0	80	8266
Qwen 2.5 1.5B	16.3	0	0	50	2350
Qwen2 0.5B Tiny	18.8	7.7	0	50	2454

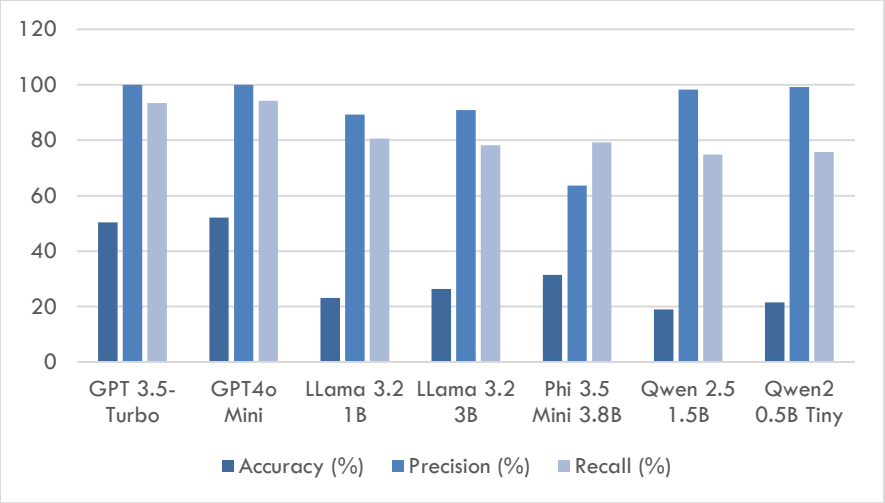

Figure 13. Comparative evaluation of model performance across the benchmark, reporting overall accuracy, syntactic precision, and functional recall. It is worth noting the ability for a small model for complex tasks degrades based on the required context injection.

4.3. Case Studies and Applications

The following case studies illustrate the system in practical use and its application to common hydrological questions. Evaluations were conducted using Mozilla Firefox, which represents one of the more constrained execution environments among the supported browser platforms due to limitations associated with several underlying technologies. These examples emphasize the system's capacity for task composition, data integration, and visualization using publicly available datasets. Both case studies are found as examples within the platform, and their corresponding web applications can be found on the platform and the workflows on the supplementary materials.

4.3.1. Case Study #1: Streamflow Response to Precipitation Events

This case study demonstrates the application of HydroBlox towards the assessment of streamflow to precipitation responses in the Iowa River Basin using publicly accessible, daily-resolution hydrometeorological datasets. The aim is to identify and quantify lag times, runoff ratios, and hydrograph recession behavior for short-term storm events, climatological assessment, and extreme event identification along with flashiness categorization.

The analytical framework is based on methods for event-based hydrologic responses as found in Morin et al. (2001), Gaál et al. (2015), and DeFries & Eshleman (2004). Daily precipitation data is retrieved using HydroLang from the NOAA Global Historical Climatology Network – Daily (GHCND) dataset (Applequist et al., 2024). Eleven precipitation stations were selected within a ~20 km radius of the streamflow station used for the analysis, in the Iowa City River network. Using the CUAHSI WaterML (Valentine et al., 2007) data sources for enabling spatial filtering in a bounding box of 41.50–41.75°N, −91.70 to −91.40°W. The same resource was used to obtain precipitation values. The following stations were queried and data retrieved between January 1950 and January 2023. The station names can be found in the supplementary materials and were chosen based on data completeness and geographic relevance. Daily precipitation totals were spatially

averaged to produce a representative rainfall signal for the basin. Concurrently, daily mean streamflow data were obtained from the USGS National Water Information System station 05454500 – Iowa River at Iowa City (USGS, 2023).

Precipitation events were defined using a multi-stage statistical signal processing pipeline designed to filter noise and enforce spatiotemporal consistency. We computed the following response metrics using the block-based functionalities: i) adaptive baseflow separation & detection - initial event candidates were detected at the station level using a rolling quantile filter. A 30-day centered window was used to estimate the hydrologic baseline (0.2 quantile), which was subtracted from the observed signal to derive the storm excess. Significant events were identified dynamically where the excess exceeded 2σ above the local variance for a minimum duration of two consecutive days; ii) regional spatiotemporal clustering - to isolate basin-wide systems from localized convective storms, a regional matching algorithm was applied. Station-level events were sorted and clustered temporally, a valid regional event was defined only when detected simultaneously (within a 2-day lag window) at a minimum of two distinct monitoring stations.

Associated streamflow responses were tracked over a ten-day post-rainfall window. To address standard storm characteristics, extreme events, and basin flashiness, we computed the following response metrics and classification strategies:

Lag time: time difference (in days) between the center of mass of the rainfall event and the streamflow peak. The formula (Eq. 1) used for these calculations

$$T_{lag} = t_{peak,Q} \frac{\sum t_i P_i}{\sum P_i} - t_{storm\ start} \quad \text{Eq. 1}$$

Runoff ratio: the ratio of direct runoff volume (discharge above baseflow) to precipitation volume during the event (Eq. 2). By integrating the daily flow rates over the event duration and normalizing against the total precipitation volume over the drainage area (8472 km2) this metric provides a dimensionless efficiency value.

$$RR = \frac{V_{streamflow}}{V_{precipitation}} = \frac{\sum Q}{\sum P_{excess} A_{basin}} \quad \text{Eq. 2}$$

Recession duration: time interval following peak discharge until flow returns to near pre-event levels (Eq. 3), calculated specifically on the recession limb of the hydrograph.

$$T_{rec} = t_{(Q \leq 0.5 Q_{peak})} - t_{peak\ flow} \quad \text{Eq. 3}$$

Climatological Assessment & Extreme Storm Identification: To separate typical short-term storms from extreme events, a climatological assessment was quantified by evaluating event duration, total regional precipitation, peak daily precipitation, and spatial footprint (number of active stations). Extreme storms were dynamically identified as the upper-tier events—characterized by substantially longer durations (averaging ~11 days compared to ~4.7 days for standard storms) and significant cumulative precipitation (averaging ~520 mm versus ~98.5 mm for baseline events) across the network.

Flashiness Categorization: To categorize the flashiness of the basin's response, a multivariate classification was applied to each event. This categorization was quantified using a combination of the calculated lag times, runoff efficiencies Rc, and the hydrograph's rise rate r_q (the rate of change in discharge leading up to the peak) as $C(E) = f(T_{lag}, R_c, r_q)$. Under this framework, Flash Floods represent the upper bound of response intensity, defined by the intersection of acute lag times ($L_t \leq 1$ day) and maximum volumetric acceleration (high r_q). Slow Basin Responses represent the lower bound, exhibiting extended lag periods ($L_t \gg 1$) and minimum r_q values indicative of highly attenuated channel routing.

These computations were performed using the hydro, stats, and python code blocks modules in combination with rolling window smoothing, peak detection, and volume integration blocks. All outputs were visualized using the visualizing components with the charting tools allowing rainfall blocks and streamflow to be plotted simultaneously with event annotations. The block definition of these items is shown in Figure 14, and results in Figure 15. Moreover, the results of the case study are available in the library examples for testing and expansion into other locations. The total execution time for the code execution was 184.2s with total size of 318.9MB.

During the analysis period for all the stations with events overlapping, a total of 1,367 events were identified with 918 being used after QA/QC filtering. Moreover:

- Average lag time: ~ 6.10 days, capturing highly variable response windows.
- Normalized runoff ratios: spanning 0 to 3.82. with a mean of 0.33.
- Flood response categorization (Flashiness): Of the 918 analyzed events, 351 were classified as Slow Basin Responses, 338 as Quick Responses, 177 as Delayed Responses, and 52 as Flash Floods.
- Extreme Event Isolation: 46 of the total events were isolated as extreme climatological events.
- Recession durations: averaged 6.62 days after peak flow.

These values contrast with regional literature, where 1-4 days lags and relatively low runoff efficiencies have been observed in similar Midwestern basins (Schilling et al, 2008; Zhanf et al., 2014). The statistical detection method effectively captured high-intensity response events (Max Response 3.82), illustrating the non-linear relationship between precipitation magnitude, basin flashiness and discharge.

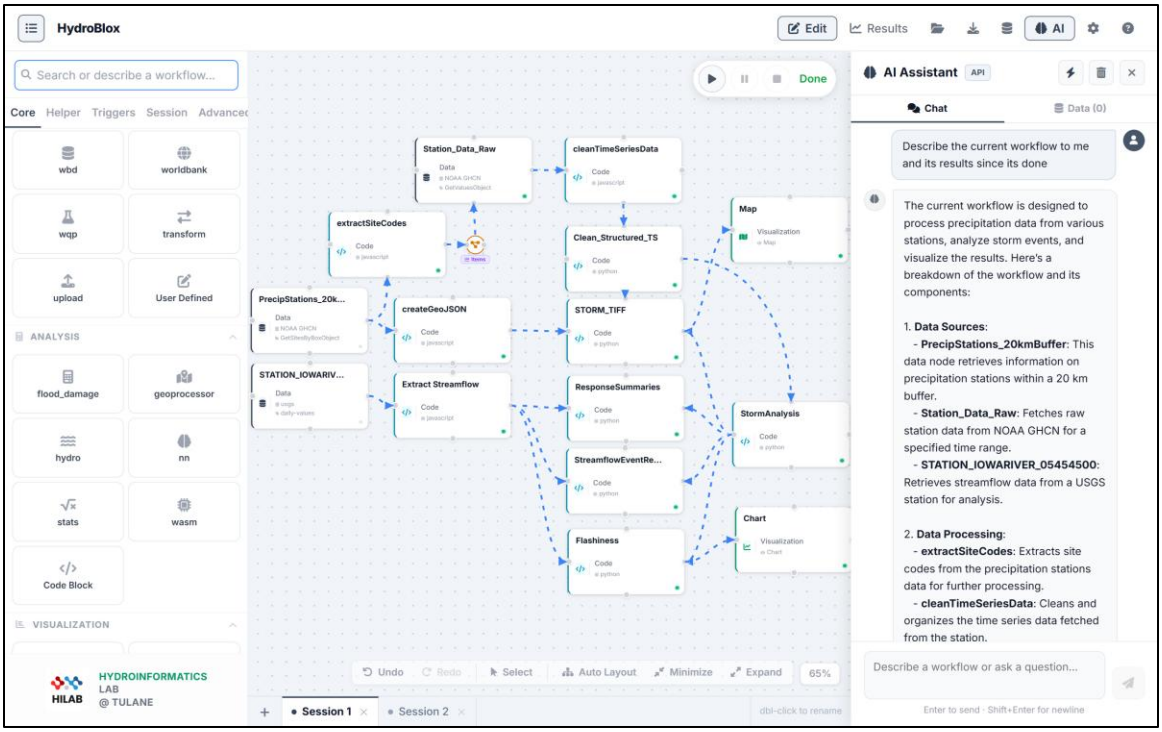

Figure 14. Block definition for case study 1.

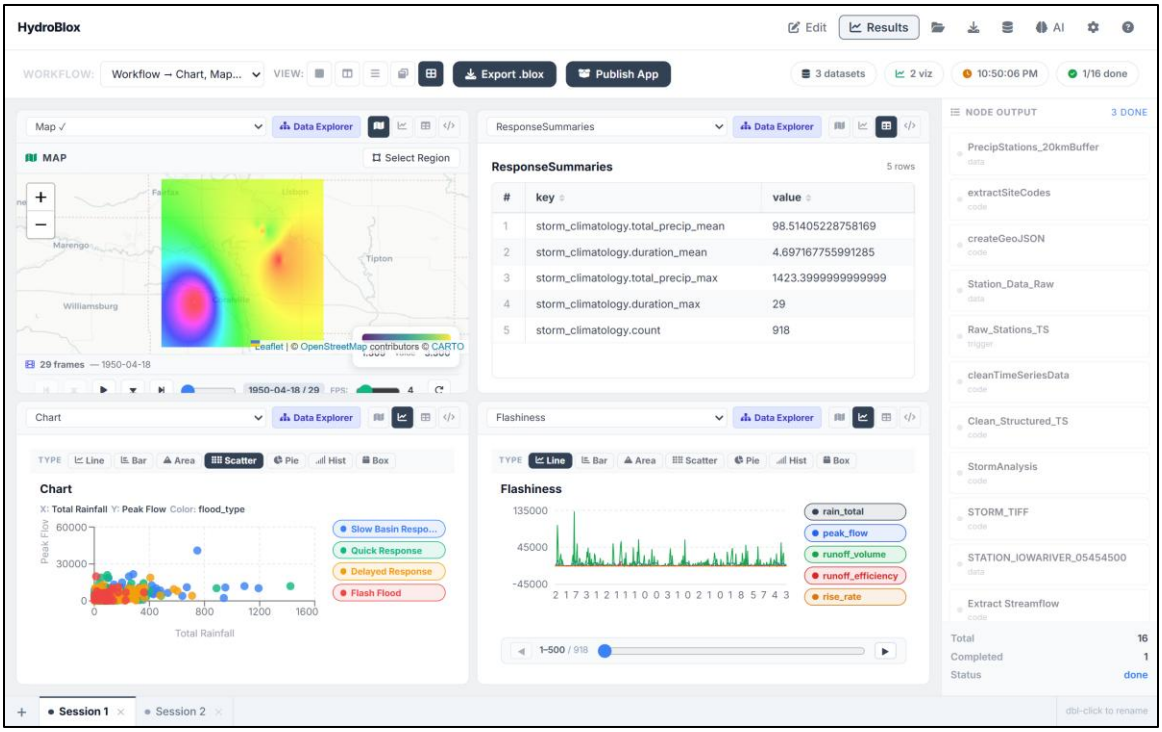

Figure 15. Result space for the case study, with the dynamic output of the charts and station locations (upper) and the results of a sample station with precipitation and streamflow outputs (lower), both with a summary statistic of the identified events.

4.3.2. Case Study #2: Drought Monitoring

Droughts are complex and gradual phenomena with widespread environmental and socioeconomic impacts. Their detection and quantification rely on robust indicators that capture multi-scale precipitation anomalies. Among these, the Standardized Precipitation Index (SPI) is widely recognized for its simplicity, probabilistic interpretability, and flexibility across temporal scales (McKee et al., 1993; WMO, 2012). SPI is based solely on precipitation and can identify meteorological drought conditions over various durations (e.g. 1-month to 24-month time scales), making it suitable for agricultural, hydrological and climatological assessments.

This study presents a multi-scale drought assessment in southeastern Iowa using monthly precipitation data from NOAA GHCN stations, covering the 1980s through 2023. The analysis quantifies drought frequency, cumulative severity, and long-term trends across 1-, 3-, 6-, and 12-month accumulation periods. All analyses were conducted within the HydroBlox client-side environment. Statistical processing—including SPI computation, drought event identification, and non-parametric trend analysis—was performed using R packages such as SPEI, Kendall, and trend. Spatial processing and map generation were implemented in Python using NumPy, GeoPandas, SciPy, and Rasterio, where station-level annual drought severity was interpolated to a regular grid and exported as rasters in 0.02deg. Data cleaning, temporal alignment, and interactive rendering were handled through HydroSuite blocks, enabling coordinated preprocessing, visualization, and export entirely on the client side. The workflow construction and execution for the analysis is shown in Figures 16 and 17. The total execution time was 274.85s with total size of 231MB.

Drought was quantified using the SPI computed for accumulation scales $t = 1,3,6,12$ months. For a given scale t, cumulative precipitation $X_t$was fit to a gamma distribution and transformed to a standard normal variate:

$$SPI_t = \Phi^{-1}(F_\Gamma(X_t)), \qquad \text{Eq. 4}$$

where $F_\Gamma$is the cumulative fitted gamma distribution and $\Phi^{-1}$is the inverse standard normal function. This probabilistic normalization ensures that SPI values are comparable across stations with differing climatologies. The use of multiple accumulation scales enables explicit separation between short-term meteorological droughts (SPI-1, SPI-3) and longer-term hydrological droughts (SPI-6, SPI-12). Droughts were treated as discrete events. A drought event was defined as one or more consecutive months where $SPI_t \leq -1$. For each event, duration D and cumulative severity S were computed as (Eq. 5):

$$S = \sum_{i=1}^{D} |\, SPI_i \,|, \qquad \text{Eq. 5}$$

Station-level drought frequency was normalized by record length. Long-term changes in drought conditions were evaluated using the Mann-Kendall test and Sen's slope estimate. To maintain physical interpretability within the pipeline, SPI series were sign-inverted so that positive trends indicate increasing drought severity. Statistical significance was evaluated at $\alpha = 0.05$.

Finally, a stochastic ensemble framework was used to generate probabilistic drought scenarios for SPI-12. Observed station SPI time series were propagated forward using a first-order autoregressive (AR1) process $X_t = \phi X_{t-1} + \epsilon_t$ where ϕ represents the temporal persistence estimated from the valid station network, and ϵ_t is a stochastic innovation term. Simulated station responses were spatially interpolated using IDW, while spatially correlated noise fields—generated via kernel smoothing of Gaussian perturbations—were added to reproduce realistic regional variability. This framework produced an ensemble of 50 simulations over multiple steps, enabling the calculation of drought probability maps. Moreover, considering the block construction, it can be adopted to other regions having constraints solely to spatial location and temporal span. The results highlight that across southeastern Iowa, the mean number of drought events decreases with the increasing SPI scale as shown in Table 4. Moreover, the nearly five-fold reduction in SPIs demonstrate the filtering effect of temporal aggregation and confirms that drought persistence dominates at longer timescales. Table 5 highlights severity and drought frequency per averaged SPI's across stations. Although the event frequency declines with scales, the severity remains substantial at longer aggregated SPI's, showing that prolonged periods of moisture deficit hydrologically relevant for southeastern Iowa.

Table 4. Mean number of droughts per station. The values were extracted from the final drought count per SPI scale.

SPI Scale	Mean Number of Droughts per Station
SPI-1	42.57
SPI-3	25.44
SPI-6	18.04
SPI-12	11.45

Table 5. Normalized drought frequency and cumulative severity per station.

SPI Scale	Mean Frequency (events/month)	Mean Cumulative Severity
SPI-1	0.1123	83.15
SPI-3	0.069	79.55
SPI-6	0.05	79.46
SPI-12	0.031	75.88

The proportion of stations exhibiting statistically significant drying trends and the corresponding Sen's slopes are shown in Table 6. Drying trends increase with temporal scale, indicating that multi-year drought conditions are intensifying more consistently than short-term variability. This framework integrates probabilistic SPI formulation, event-based extraction, and non-parametric trend estimation to capture drought frequency, persistence, and severity. Results from the HydroBlox client-side analysis in southeastern Iowa identify frequent meteorological anomalies and increasingly persistent hydrological droughts throughout the historical record. Sign-inverted Mann-Kendall tests and Sen's slope estimates indicate emerging regional drying, consistent with broader Midwestern hydrological studies (McKee et al., 1993; Svoboda et al., 2002; WMO, 2012; Fuchs et al., 2014). Although currently limited to precipitation-only inputs and

station-based interpolation, the modular HydroSuite architecture supports extension to multi-variable indices and advanced spatial modeling for scalable hydroclimatic risk assessments.

Table 6. Stationwide proportion exhibiting statistically significant drying trends increases monotonically with SPI scale.

SPI Scale	% Drying Stations	% Wetting Stations	Mean Sen's Slope
SPI-1	50	16.67	-0.0012
SPI-3	58.06	22.58	-0.0015
SPI-6	51.22	21.43	-0.0017
SPI-12	60.98	20	-0.0021

5. Discussions and Limitations

5.1. Contributions and Broader Impact

HydroBlox represents an advancement in browser-based hydroinformatics, offering a visual environment for constructing reproducible analytical pipelines without the need for backend infrastructure. Grounded in the HydroSuite ecosystem, the platform decouples the user interface from the underlying computational logic. This modular architecture allows users to assemble workflows using standardized functional blocks while ensuring that the system remains extensible; third-party tools and custom algorithms can be integrated dynamically without requiring modifications to the core application kernel.

Technically, the platform validates the feasibility of a client-side runtime that accommodates diverse methodological needs. By integrating Pyodide and WebR, HydroBlox enables the direct execution of Python and R scripts within custom code blocks, allowing researchers to leverage existing statistical libraries alongside visual components. This architecture supports custom item handlers, enabling the ingestion of proprietary or non-standard data formats directly in the browser. Furthermore, the inclusion of AI-assisted workflow generation lowers the technical barrier to entry, guiding users through block selection, logic definition, and parameter tuning. Together, these features establish a zero-install research environment that facilitates rapid prototyping and educational accessibility, providing a scalable blueprint for open science in hydrology.

5.2.Validation and Impact Evidence

The practical utility of the framework was validated during the IAHR training course on No-Code Visual Programming for Hydrology during December 8–12, 2025 (IAHR, 2025), which engaged a global cohort of practitioners. Analysis of the participant demographics (378 registered) indicates a diverse user base dominated by academia (68.97%) and consulting sectors (17.24%), with significant representation from water utilities and public administration (13.8%) (Figure 18). The platform successfully lowered technical entry barriers for a wide range of expertise levels; 27.59% of users identified as beginners in hydroinformatics, while the majority were intermediate (48.28%) or advanced (20.69%) practitioners, confirming the system's adaptability to varying skill sets.

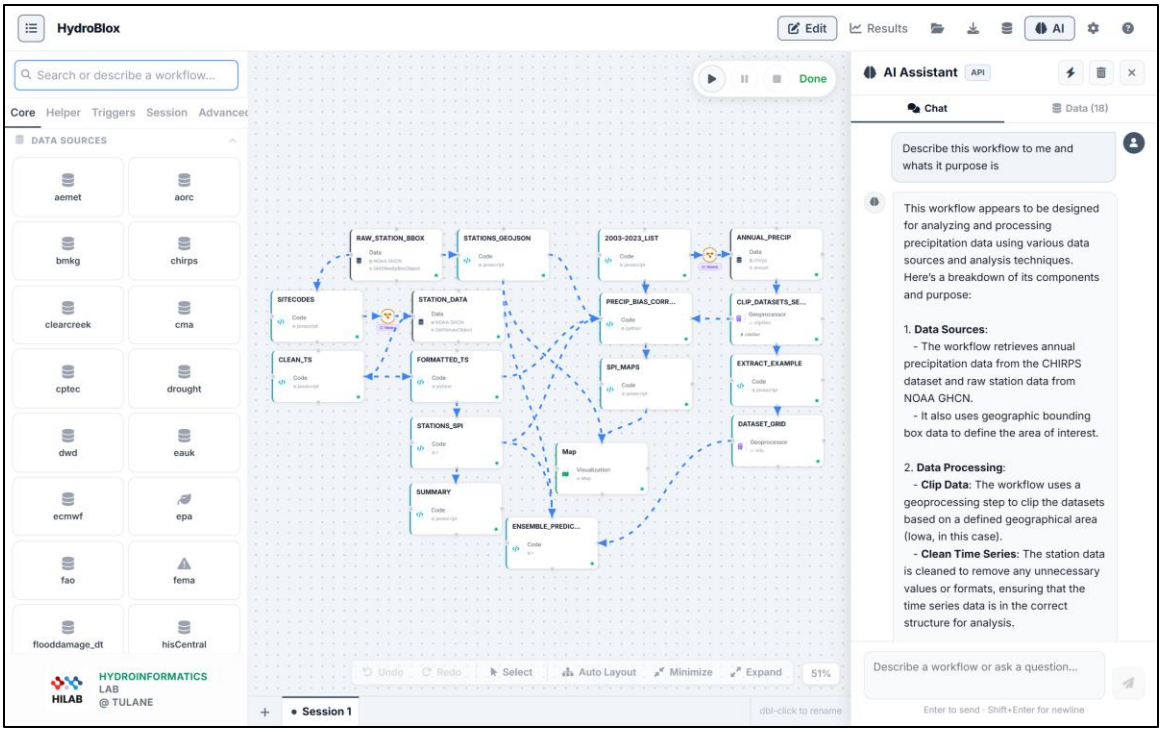

Figure 16. Block definition for case study 2.

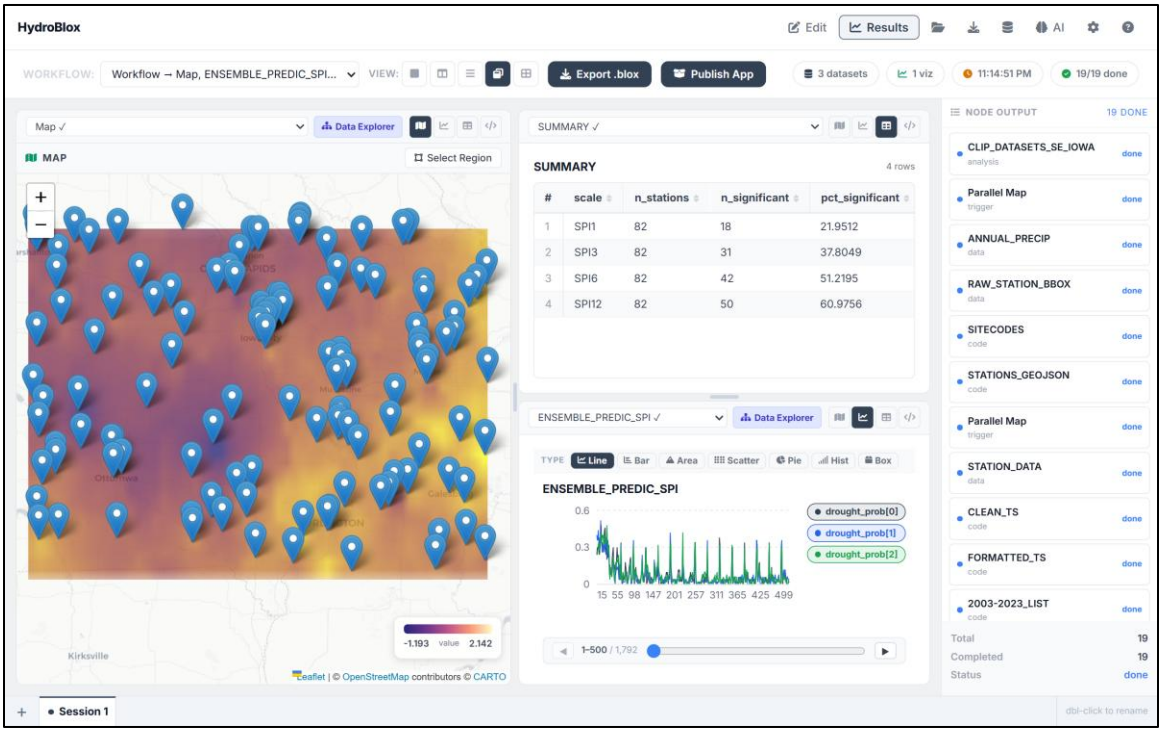

Figure 17. Integrated drought analysis outputs generated in the HydroBlox results interface for southeastern Iowa, including spatial drought severity maps, station-level SPI time series, statistical trend summaries, and mean drought counts across SPI timescales.

Quantitative indicators from the post-event evaluation demonstrate high system efficacy and user satisfaction. When rating the new initiative, 95.24% of respondents categorized it as excellent (57.14%) or very good (38.10%) (Figure 19). Similarly, the overall course quality was rated as excellent or very good by 76.92% of participants. Usability metrics further validated the workflow design, with 84.00% of respondents affirming that the platform successfully balanced theoretical concepts with practical application. Qualitative feedback highlighted specific areas for future optimization, including requests for more detailed step-by-step guidelines on working examples and the expansion of analysis blocks to cover AI applications in poorly gauged basins and operational forecasting for water infrastructure. These community-driven insights are currently guiding the development of the next iteration of the execution engine.

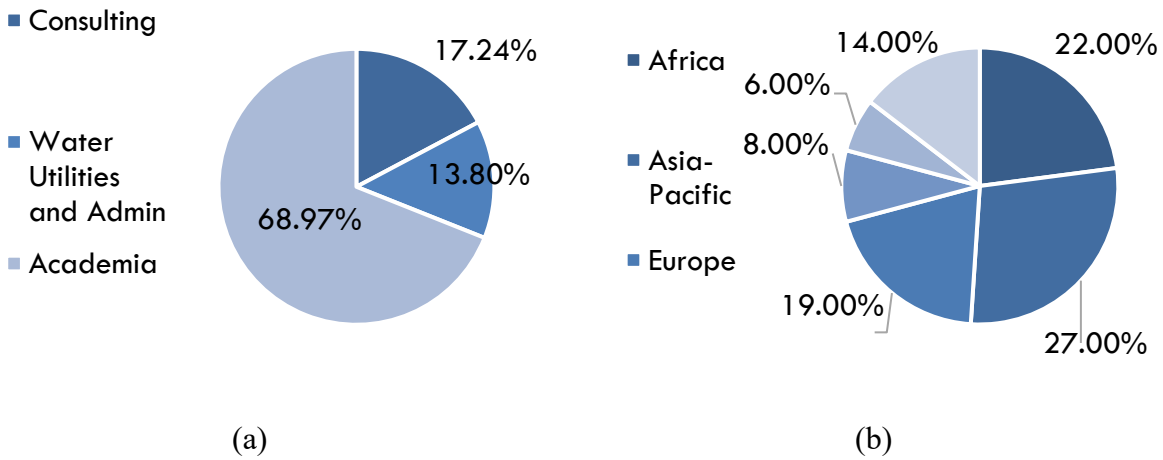

(a) (b)

Figure 18. (a) Groups that joined the training and (b) represented geographic groups.

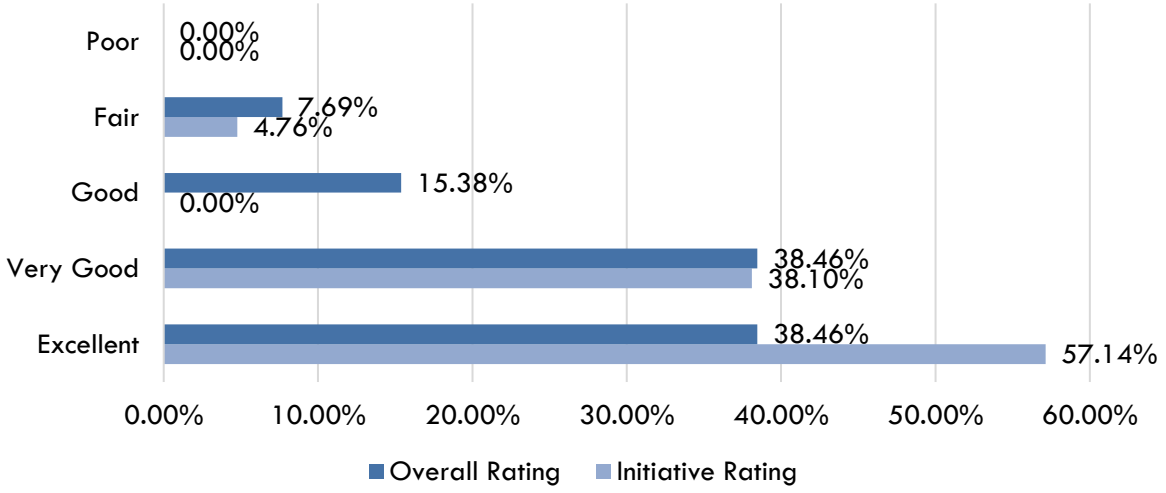

Figure 19. Overall results of the tool used, and the initiative being brought forward during the training. This includes the use of visual blocks, connections to data sources and uses, and the integration of AI for block generation and analysis.

5.3. Limitations

While HydroBlox provides a functional client-side research environment, users are constrained by the browser architecture and the current maturity of the ecosystem. The most immediate limitation arises from the computational ceiling imposed by the browser's memory sandbox. Unlike native desktop applications that benefit from virtual memory, disk-backed caching, and multi-process execution, HydroBlox operates within the fixed memory allocation available to a single browser context, typically on the order of 2–4 GB. Although the platform supports a broad range of analytical workflows—including statistical analysis and geospatial manipulation—this memory ceiling becomes restrictive for large datasets, particularly when working with long temporal records or high-resolution gridded products. In practice, users must often constrain the spatial or temporal extent of their analyses or explicitly decompose datasets into smaller subsets to remain within the available memory footprint. A standalone desktop distribution of HydroBlox is currently under development as an alternative deployment mode, lifting the browser-imposed constraints by executing Python and R workflows natively against the host system's full resource envelope; however, this avenue remains secondary to the platform's primary web-based delivery model.

Beyond resource limitations, workflow execution in HydroBlox remains subject to browser compatibility and security constraints. Certain scientific libraries and system-level dependencies commonly used in desktop environments are not yet available within a browser context. While emerging technologies such as WASM offer potential pathways to expand library support, these approaches remain an area for future exploration rather than a fully realized solution. At present, the platform mitigates some of these constraints through dynamic content delivery and modular dependency loading, allowing incremental adoption of browser-compatible scientific tooling as it matures.

Additional challenges stem from the integration of a local-first AI assistant and the flexibility of the visual workflow canvas. The use of localized, quantized language models ensures data privacy and low-latency interaction but introduces trade-offs in reasoning depth and domain specificity. These models may produce incomplete or imprecise logic when generating complex workflows or recalling specialized parameter conventions, requiring users to manually review and validate generated outputs. Similarly, the expressive power of the visual programming environment introduces the risk of constructing workflows that are logically valid yet computationally unstable, such as implicit circular dependencies or unresolved data type mismatches. Such issues may lead to silent failures or execution crashes, occasionally requiring a full page reload and loss of transient state. Although safeguards exist to reduce these risks, overall performance remains bounded by the capabilities of the user's hardware.

Finally, the scalability of HydroBlox is inherently limited by the diversity of hydrological science itself. While the platform supports a substantial subset of commonly used analyses and data sources, it cannot comprehensively include every specialized model or domain-specific tool. Addressing this limitation requires a community-driven extension approach, in which users contribute additional functionality as modular components. However, this introduces a barrier for

practitioners who lack the technical expertise needed to package and integrate custom tools within the HydroBlox architecture. Future development will therefore depend on improved interoperability standards, simplified extension mechanisms, and governance structures that maintain scientific rigor while lowering the barrier to community contribution.

6. Conclusions

This work presents HydroBlox, a web-based platform for constructing, executing, and sharing hydrological workflows using a visual programming paradigm. Built entirely on client-side technologies, the system supports modular integration of data sources, analytical functions, and visualization components through a structured, block-based interface. It enables users to define and modify workflows interactively, with no requirement for server infrastructure or programming expertise.

Through its integration with the HydroSuite library ecosystem and support for WebAssembly execution, HydroBlox supports both general-purpose hydrological processing and advanced, domain-specific computation with potential hooks and integrations to legacy desktop applications and python libraries in hydrology. The inclusion of an AI-assisted interface further enhances the modeling experience by providing contextual suggestions and reducing the effort needed to assemble valid workflows.

The case studies demonstrate that the system is capable of supporting real-world hydrological analyses, including event-based streamflow response assessment and drought index calculation. Results can be visualized within the platform and exported as reproducible, portable applications for further use, instruction, or archiving. By focusing on browser-native deployment and structured, user-centered workflow generation through recipes within the context of the platform, HydroBlox provides a foundation for rethinking how environmental models and analyses are built, shared, and sustained in hydrological science.

Acknowledgements

This material is based upon work supported by the Department of Interior (DOI) - US Geological Survey (USGS) under Award No. G25AP00137.

Declaration of generative AI and AI-assisted technologies in the writing process

During the preparation of this work the author(s) used ChatGPT and Claude in order to develop the software herein described and improve readability throughout the manuscript. After using this tool/service, the author(s) reviewed and edited the content as needed and take(s) full responsibility for the content of the publication.

CRediT Statement

Carlos Erazo Ramirez: Conceptualization, Data curation, Formal analysis, Investigation, Methodology, Software, Visualization, Writing – original draft. Ibrahim Demir:, Conceptualization, Funding acquisition, Methodology, Project Administration, Supervision, Writing – review & editing.

7. References

Agliamzanov, R., Sit, M., & Demir, I. (2020). Hydrology@ Home: a distributed volunteer computing framework for hydrological research and applications. *Journal of Hydroinformatics*, *22*(2), 235-248.

Almoradie, A., Popescu, I., Jonoski, A., & Solomatine, D. (2013). Web based access to water related data using OGC WaterML 2.0. *International Journal of Advanced Computer Science and Applications*, *3*(3). https://doi.org/10.14569/specialissue.2013.030310

Alvioli, M., & Baum, R. (2016). Parallelization of the TRIGRS model for rainfall-induced landslides using the message passing interface. *Environmental Modelling & Software*, *81*, 122-135. https://doi.org/10.1016/j.envsoft.2016.04.002

Applequist, S., Durre, I., & Vose, R. (2024). The Global Historical Climatology Network Monthly Precipitation Dataset, Version 4. *Scientific Data*, *11*(1), 633.

Burian, S. J., Cohen, S., Halgren, J., & Johnson, R. C. (2023, January). Strategies of NOAA's Cooperative Institute for Research to Operations in Hydrology (CIROH) to Accelerate Research Community Advances into Operational Water Prediction Practice. In American Meteorological Society Meeting Abstracts (Vol. 103, pp. PD9A-3).

Cushing, L., Morello-Frosch, R., Wander, M., & Pastor, M. (2015). Toward the next generation of climate and environmental justice research: integrating science, policy, and community. Environmental Research Letters, 10(2), 025017. https://doi.org/10.1088/1748-9326/10/2/025017

Deelman, E., Gannon, D., Shields, M., & Taylor, I. (2009). Workflows and E-SciEncE: An overview of workflow system features and capabilities. Future Generation Computer Systems, 25(5), 528-540. https://doi.org/10.1016/j.future.2008.06.012

DeFries, R. S., & Eshleman, K. N. (2004). Land-use change and hydrologic processes: A major focus for the future. Hydrological Processes, 18(11), 2183–2186. https://doi.org/10.1002/hyp.5584

Demir, I., & Szczepanek, R. (2017). Optimization of river network representation data models for web-based systems. *Earth and Space Science*, *4*(6), 336-347.

Erazo Ramirez, C., Sermet, Y., & Demir, I. (2023). HydroLang markup language: Community-driven web components for hydrological analyses. Journal of Hydroinformatics, 25(4), 1171-1187. https://doi.org/10.2166/hydro.2023.149

Erazo Ramirez, C., Sermet, Y., & Demir, I. (2024). HydroCompute: An open-source web-based computational library for hydrology and environmental sciences. Environmental Modelling & Software, 175, 106005. https://doi.org/10.1016/j.envsoft.2024.106005

Erazo Ramirez, C., Sermet, Y., Molkenthin, F., & Demir, I. (2022). HydroLang: An open-source web-based programming framework for hydrological sciences. Environmental Modelling & Software, 157, 105525. https://doi.org/10.1016/j.envsoft.2022.105525

Essawy, B. T., Goodall, J. L., Zell, W., Voce, D., Morsy, M. M., Sadler, J., Yuan, Z., & Malik, T. (2018). Integrating scientific cyberinfrastructures to improve reproducibility in computational

hydrology: Example for HydroShare and GeoTrust. Environmental Modelling & Software, 105, 217–229. https://doi.org/10.1016/j.envsoft.2018.03.025

Ewing, G., Erazo Ramirez, C., Vaidya, A., & Demir, I. (2024). Client-side web-based model coupling using basic model interface for hydrology and water resources. *Journal of Hydroinformatics*, *26*(2), 494-502.

Feltrin, L. (2015). KNIME an open source solution for predictive analytics in the geosciences [software and data sets]. IEEE Geoscience and Remote Sensing Magazine, 3(4), 28-38.

Feng, G., & Yan, W. (2024). Text2VP: Generative AI for Visual Programming and Parametric Modeling. *arXiv preprint arXiv:2407.07732*.

Finkenbiner, C., & Semmendinger, D. (2021). Visualization workflow for quantifying parameter sensitivities and uncertainties for hydrologic models. JAWRA Journal of the American Water Resources Association, 57(5), 731–744. https://doi.org/10.1111/1752-1688.12946

Gaál, L., Molnar, P., & Szolgay, J. (2015). Selection of intense rainfall-runoff events in mesoscale catchments for flash flood modeling. Hydrology and Earth System Sciences, 19(8), 3567–3585. https://doi.org/10.5194/hess-19-3567-2015

GDAL/OGR (2023). *GDAL: Geospatial Data Abstraction Library* (Version 3.x) [Computer software]. Open Source Geospatial Foundation. https://gdal.org

Gil, Y., Deelman, E., Ellisman, M., Fahringer, T., Fox, G., Gannon, D., Goble, C., Livny, M., Moreau, L. and Myers, J., (2007). Examining the challenges of scientific workflows. Computer, 40(12), pp.24-32.

Gil, Y., David, C.H., Demir, I., Essawy, B.T., Fulweiler, R.W., Goodall, J.L., Karlstrom, L., Lee, H., Mills, H.J., Oh, J.H. and Pierce, S.A., (2016). Toward the Geoscience Paper of the Future: Best practices for documenting and sharing research from data to software to provenance. Earth and Space Science, 3(10), pp.388-415.

Haas, A., Rossberg, A., Schuff, D. L., Titzer, B. L., Holman, M., Gohman, D., Wagner, L., Zakai, A., & Bastien, J. (2017). Bringing the web up to speed with WebAssembly. Proceedings of the 38th ACM SIGPLAN Conference on Programming Language Design and Implementation. https://doi.org/10.1145/3062341.3062363

Haristiani, N. (2019). Artificial intelligence (AI) chatbot as language learning medium: An inquiry. Journal of Physics: Conference Series, 1387(1), 012020. https://doi.org/10.1088/1742-6596/1387/1/012020

Horsburgh, J. S., Morsy, M. M., Castronova, A. M., Goodall, J. L., Gan, T., Yi, H., Stealey, M. J., & Tarboton, D. G. (2015). HydroShare: Sharing diverse environmental data types and models as social objects with application to the hydrology domain. JAWRA Journal of the American Water Resources Association, 52(4), 873-889. https://doi.org/10.1111/1752-1688.12363

Hume, D. A. (2017). *Progressive web apps*. Manning.

Hut, R. W., Hutton, C., Drost, N., van de Giesen, N., & Savenije, H. H. G. (2022). The eWaterCycle platform for open and FAIR hydrological collaboration. Geoscientific Model Development, 15, 5371–5387. https://doi.org/10.5194/gmd-15-5371-2022

Hutton, C., Wagener, T., Freer, J., Han, D., Duffy, C., & Arheimer, B. (2016). Most computational hydrology is not reproducible, so is it really science? Water Resources Research, 52(10), 7548–7555. https://doi.org/10.1002/2016WR019285

Hutton, E., Piper, M., & Tucker, G. (2020). The basic model interface 2.0: A standard interface for coupling numerical models in the geosciences. *Journal of Open Source Software*, *5*(51), 2317. https://doi.org/10.21105/joss.02317

HydroSuite, 2004. Github repository at https://github.com/uihilab/HydroSuite.

IAHR. (2025, October 29). IAHR training course on no-code visual programming for hydrology: AI-enabled web platforms and open-source tools for research and education. https://www.iahr.org/index/detail/2104

Karris, S. T. (2006). Introduction to Simulink with engineering applications. Orchard Publications.

Kizilkaya, D., Sajja, R., Sermet, Y., & Demir, I. (2025). Toward HydroLLM: a benchmark dataset for hydrology-specific knowledge assessment for large language models. *Environmental Data Science*, *4*, e31.

Kodosky, J. (2020). LabVIEW. Proceedings of the ACM on Programming Languages, 4(HOPL), 1-54.

Kuhail, M. A., Sakr, M., Benatallah, B., & Casati, F. (2021). Visual programming languages in data science and machine learning: A systematic literature review. Journal of Systems and Software, 179, 111035. https://doi.org/10.1016/j.jss.2021.111035

Maghami, I., Morsy, M.M., Sadler, J.M., Horsburgh, J.S., Dash, P.K., Choi, Y., Chen, K., Seul, M., Black, S., Tarboton, D.G., Goodall, J.L., 2024. An extensible schema for capturing environmental model metadata: Implementation in the HydroShare online data repository. Environmental Modelling & Software, 140, 105041. https://doi.org/10.1016/j.envsoft.2023.105895

McKee, T. B., Doesken, N. J., & Kleist, J. (1993). The relationship of drought frequency and duration to time scales. 8th Conference on Applied Climatology, 17(22), 179–183.

Merwade, V., & Ruddell, B. L. (2012). Moving university hydrology education forward with community-based geoinformatics, data and modeling resources. *Hydrology and Earth System Sciences*, *16*(8), 2393-2404.

Mishra, A., Bansal, D., & Jain, S. (2023). LLMs for scientific workflow synthesis: A survey. arXiv preprint arXiv:2302.01726. https://doi.org/10.48550/arXiv.2302.01726

Moges, E., Ruddell, B. L., Zhang, L., Driscoll, J. M., Norton, P., Perez, F., & Larsen, L. G. (2022). HydroBench: Jupyter supported reproducible hydrological model benchmarking and diagnostic tool. *Frontiers in Earth Science*, *10*. https://doi.org/10.3389/feart.2022.884766

Morin, J., Benyamini, Y., Michaeli, A., & Yair, A. (2001). Rainfall and runoff in the arid Negev of Israel: Patterns and processes. Catena, 45(1), 1–25. https://doi.org/10.1016/S0341-8162(01)00132-6

Ooms, J. (2024). *WebR: R in the browser* [Computer software]. The R Project for Statistical Computing. https://docs.r-wasm.org/webr/

Perkel, J. M. (2023). The AI assistants are here. Nature, 611(7937), 192–195. https://doi.org/10.1038/d41586-022-03627-7

Pursnani, V., Ramirez, C. E., Sermet, M. Y., & Demir, I. (2024). HydroSuite-AI: Facilitating Hydrological Research with LLM-Driven Code Assistance. *EarthArxiv*, 8121. https://doi.org/10.31223/X5RM6Q

Pursnani, V., Sermet, Y., & Demir, I. (2025). A conversational intelligent assistant for enhanced operational support in floodplain management with multimodal data. *International Journal of Disaster Risk Reduction*, 122, 105422.

Pyodide (2024). *Pyodide: Python scientific computing in the browser* [Computer software]. https://pyodide.org

Ramirez, C. E., Sermet, Y., Shahid, M., & Demir, I. (2024). HydroRTC: A web-based data transfer and communication library for collaborative data processing and sharing in the hydrological domain. *Environmental Modelling & Software*, *178*, 106068.

Ridler, M. E., Van Velzen, N., Hummel, S., Sandholt, I., Falk, A. K., Heemink, A., & Madsen, H. (2014). Data assimilation framework: Linking an open data assimilation library (OpenDA) to a widely adopted model interface (OpenMI). *Environmental Modelling & Software*, *57*, 76-89. https://doi.org/10.1016/j.envsoft.2014.02.008

Ruiz-Pérez, G., et al. (2016). Investigating the behaviour of a small Mediterranean catchment using three different hydrological models as hypotheses. Hydrological Processes, 30(25), 4632–4647. https://doi.org/10.1002/hyp.10738

Sajja, R., Pursnani, V., Sermet, Y., & Demir, I. (2025). AI-assisted educational framework for floodplain manager certification: Enhancing vocational education and training through personalized learning. *IEEE Access*, 13, 42401 - 42413.

Schilling, K. E., & Zhang, Y.-K. (2008). Baseflow contribution to nitrate-nitrogen export from a large, agricultural watershed, USA. Journal of Hydrology, 295(1–4), 305–316. https://doi.org/10.1016/j.jhydrol.2004.03.010

Sen, P. K. (1968). Estimates of the regression coefficient based on Kendall's tau. Journal of the American Statistical Association, 63(324), 1379–1389. https://doi.org/10.2307/2285891

Seo, B. C., Keem, M., Hammond, R., Demir, I., & Krajewski, W. F. (2019). A pilot infrastructure for searching rainfall metadata and generating rainfall product using the big data of NEXRAD. *Environmental modelling & software*, *117*, 69-75.

Shahid, M., Sermet, Y., Mount, J., & Demir, I. (2023). Towards progressive geospatial information processing on web systems: a case study for watershed analysis in Iowa. Earth science informatics, 16(2), 1597-1610.

Simonson, A., Brown, O., Dissen, J., Kearns, E. J., Szura, K., & Brannock, J. (2022). Noaa open data dissemination (formerly NOAA big data project/program). Big Data Analytics in Earth, Atmospheric, and Ocean Sciences, 65-94.

Sit, M., Langel, R. J., Thompson, D., Cwiertny, D. M., & Demir, I. (2021). Web-based data analytics framework for well forecasting and groundwater quality. *Science of the Total Environment*, *761*, 144121.

Stagge, J. H., Rosenberg, D. E., Abdallah, A. M., Akbar, H., Attallah, N. A., & James, R. (2019). Assessing data availability and research reproducibility in hydrology and water resources. *Scientific Data*, *6*(1). https://doi.org/10.1038/sdata.2019.30

Stolpe, O., & Hällström, P. (2023). Enhancing computational thinking in STEM education through block-based programming: A meta-analysis. Journal of Educational Computing Research, 61(3), 715–742. https://doi.org/10.1177/07356331221144180

Swain, N. R., Christensen, S. D., Snow, A. D., Dolder, H., Espinoza-Dávalos, G., Goharian, E., Jones, N. L., Nelson, E. J., Ames, D. P., & Burian, S. J. (2016). A new open source platform for lowering the barrier for environmental web app development. *Environmental Modelling & Software*, *85*, 11-26. https://doi.org/10.1016/j.envsoft.2016.08.003

Tarboton, D. G., Idaszak, R., Horsburgh, J. S., Heard, J., Ames, D., Goodall, J. L., ... & Maidment, D. (2014). HydroShare: advancing collaboration through hydrologic data and model sharing.

Tarboton, Ames, Horsburgh, Goodall, Couch, Hooper, Bales, Wang, Castronova, Seul, Idaszak, Li, Dash, Black, Ramirez, Yi, Calloway, Cogswell, 2022, *Environmental Modelling & Software*, 157, 105514). https://doi.org/10.1016/j.envsoft.2023.105902

U.S. Geological Survey. (2023a). *3D Elevation Program (3DEP)*. U.S. Department of the Interior. https://www.usgs.gov/3d-elevation-program

U.S. Geological Survey. (2023b). National Water Information System (NWIS). Retrieved from https://waterdata.usgs.gov/nwis

Valentine, D. W., Zaslavsky, I., Whitenack, T., & Maidment, D. (2007, December). Design and implementation of CUAHSI WATERML and WaterOneFlow Web services. In *AGU Fall Meeting Abstracts* (Vol. 2007, pp. IN53C-08).

Verma, T., Renu, R., & Gaur, D. (2014). Tokenization and filtering process in RapidMiner. International Journal of Applied Information Systems, 7(2), 16-18.

Wagner, A. S., Waite, L. K., Wierzba, M., Hoffstaedter, F., Waite, A. Q., Poldrack, B., ... & Hanke, M. (2022). FAIRly big: A framework for computationally reproducible processing of large-scale data. *Scientific data*, *9*(1), 80.

WMO. (2012). Standardized Precipitation Index User Guide. Geneva: World Meteorological Organization.

Zhao, Q., Yu, L., Li, X., Peng, D., Zhang, Y., & Gong, P. (2021). Progress and trends in the application of Google Earth and Google Earth Engine. Remote Sensing, 13(18), 3778.